# Cellular mechanisms underlying the effects of cilostazol, milrinone, isoproterenol and ajmaline on electrographic and arrhythmic manifestations of early repolarization syndrome, and comparative analysis of the cardiac electrophysiological effects of the optical isomers of mexiletine

**PhD Thesis**

**Bence Patocskai, MD**

**Szeged**

**2017**

**Department of Pharmacology and Pharmacotherapy,**
**Faculty of Medicine, University of Szeged,**
**Szeged, Hungary**

**Supervisor:**

**István Koncz MD, PhD**

STUDIES RELATED TO THE OBJECT OF THE THESIS

(I.) **Patocskai B**, Barajas-Martinez H, Hu D, Gurabi Z, Koncz I, Antzelevitch C. Cellular and ionic mechanisms underlying the effects of cilostazol, milrinone, and isoproterenol to suppress arrhythmogenesis in an experimental model of early repolarization syndrome. *Heart Rhythm.* 2016 Jun; 13(6):1326-34.

(II.) **Patocskai B**, Koncz I, Gurabi Z, Antzelevitch C. Cellular mechanisms underlying the effect of cilostazol, milrinone and isoproterenol to supress arrhythmogenesis in an experimental model of early repolarization syndrome. In: Program and abstracts of the *23rd Annual Meeting of the Upstate New York Cardiac Electrophysiology Society and Upper Canada Cardiac Electrophysiology Society*; October 11, 2013, Toronto, Canada

(III.) Koncz I, Gurabi Z, **Patocskai B**, Panama BK, Szél T, Hu D, Barajas-Martínez H, Antzelevitch C. Mechanisms underlying the development of the electrocardiographic and arrhythmic manifestations of early repolarization syndrome. *Journal of Molecular and Cellular Cardiology*, 2014 Mar; 68:20-8.

(IV.) **Patocskai B**, Yoon N, Antzelevitch C. Mechanisms Underlying Epicardial Radiofrequency Ablation to Suppress Arrhythmogenesis in Experimental Models of Brugada Syndrome. *Journal of the American College of Cardiology: Clinical Electrophysiology*, 2016 Dec [Epub ahead of print); DOI: 10.1016/j.jacep.2016.10.011

(V.) Gurabi Z, Koncz I, **Patocskai B**, Nesterenko VV, Antzelevitch C. Cellular mechanism underlying hypothermia-induced VT/VF in the setting of early repolarization and the protective effect of quinidine, cilostazol and milrinone.
*Circulation: Arrhythmia and Electrophysiology*, 2014 Feb;7(1):134-42.

(VI.) **Patocskai B**, Gurabi Z, Györe B, Virág L, Mátyus P, Papp JGy, Varró A, Koncz I .
Electrophysiological effects of the R- and S-enantiomers of mexiletine and their combination with sotalol in isolated canine papillary muscle.
*(Manuscript in preparation.)*

(VII.) Gurabi Z, **Patocskai B**, Györe B, Virág L, Mátyus P, Papp JGy, Varró A, Koncz I.
Different electrophysiological effects of the levo- and dextrorotatory isomers of mexiletine in isolated rabbit cardiac muscle. *Canadian Journal of Physiology and Pharmacology*. 2017 Feb. doi: 10.1139/cjpp-2016-0599. [Epub ahead of print]

(VIII.) Antzelevitch C, **Patocskai B**. Ionic and Cellular Mechanisms Underlying the J wave Syndromes. Book chapter in: *J wave syndromes. Springer International Publishing Switzerland 2016.* ISBN 978-3-319-31576-8 and ISBN 978-3-319-31578-2 (eBook)
DOI 10.1007/978-3-319-31578-2 , Library of Congress Control Number: 2016942096

(IX.) **Patocskai B**, Borbáth V, Li GR, Antzelevitch C. Acacetin Suppresses Arrhythmic and Electrocardiographic Manifestations of Brugada and Early Repolarization Syndromes. Submitted to *Journal of the American College of Cardiology: Clinical Electrophysiology. 2017.*

(X.) **Patocskai B** and Antzelevitch C. Novel therapeutic strategies for the management of ventricular arrhythmias associated with the Brugada syndrome. *Expert Opinion on Orphan Drugs*, 2015; 3(6):633-651.

(XI.) Antzelevitch C, **Patocskai B**. Brugada Syndrome: Clinical, Genetic, Molecular, Cellular, and Ionic Aspects. *Curr Probl Cardiol.* 2016 Jan;41(1):7-57. (Epub 2015 Jun 11)

(XII.) **Patocskai B**, Szél T, Yoon N, Antzelevitch C. Cellular mechanisms underlying the fractionated and late potentials on epicardial electrograms and the ameliorative effect of epicardial radiofrequency ablation in an experimental model of Brugada syndrome. In: Program and abstracts of the *24th Annual Upstate New York Cardiac Electrophysiology Society and Upper Canada Cardiac Electrophysiology Society Meeting*, November 3, 2014, Buffalo, NY

(XIII.) **Patocskai B**, Szél T, Yoon N, Antzelevitch C. Cellular mechanisms underlying fractionated and late potentials on epicardial electrograms and the ameliorative effect of epicardial radiofrequency ablation in an experimental model of Brugada syndrome. In: Program and abstracts of the *35th Annual Heart Rhythm Society Meeting* May 9, 2014 San Fransisco, CA

## OTHER STUDIES

(XIV.) El-Battrawy I, Lang S, Zhao Z, Akin I, Yücel G, Meister S, **Patocskai B**, Behnes M, Rudic B, Tülümen E, Liebe V, Tiburcy M, Dworacek J, Zimmermann WH, Utikal J, Wieland T, Borggrefe M, Zhou XB. Hyperthermia influences the effects of sodium channel blocking drugs in human induced pluripotent stem cell-derived cardiomyocytes. *PLoS One.* 2016 Nov 9;11(11):e0166143.

(XV.) El-Battrawy I, Zhao Z, Lan H, Schünemann JD, Sattler K, Buljubasic F, Gökhan Y, **Patocskai B**, Lang S, Ravens U, Nowak D, Zimmermann WH, Cyganek L, Utikal J, Wieland T, Bieback K, Borggrefe M, Akin I, Zhou XB: Estradiol protection against the toxic effects of catecholamine on electrical properties in human-induced pluripotent stem cell derived cardiomyocytes. Submitted to *Journal of the American College of Cardiology: Heart failure.* 2017.

(XVI.) El-Battrawy I, **Patocskai B**, Zhao Z, Lang S, Schünemann JD, Yücel G, Akin I, Behnes M, Tiburcy M, Dworacek J, Zimmermann WH, Utikal J, Wieland T, Borggrefe M, Zhou XB. Estradiol protection against the toxic effects of isoprenaline on electrical properties in human induced pluripotent stem cell derived cardiomyocytes. In: Program and abstracts of the *Annual DZHK (German Center for Cardiovascular Research) Retreat 2016, Partner Site Heidelberg/Mannheim,* February 26-27. 2016, Asselheim, Germany

# Table of contents

SUMMARY

***Background:***

**I.** Early Repolarization Syndrome (ERS) is characterized by J-point elevation in the lateral and/or inferolateral leads of the standard 12-lead ECG and increased vulnerability to polymorphic ventricular tachycardia (VT) and fibrillation (VF) leading to sudden cardiac death. According to recent discoveries in this field, the phosphodiesterase-3 (PDE-3) inhibitor cilostazol may be a promising candidate to combat ERS-related VT/VF; whereas the Class I/A sodium channel ($I_{Na}$) blocker ajmaline exerts mild suppression on the electrocardiographic pattern of the syndrome (ERP), despite its unmasking effect on the other J wave syndrome congener, Brugada syndrome (BrS).

**II.** Lately, the Class I/B $I_{Na}$ blocker mexiletine has attracted attention afresh, due to its recently described potency to effectively terminate acquired long QT syndrome-related torsades de pointes (TdP) tachyarrhythmias and its lately emerged application opportunities in the therapy of certain neurologic and myotonic disorders. Studies directed to exhaustive comparison of the effects of mexiletine's R-(-) and S-(+) optical isomers on the action potential duration (APD) of cardiac ventricular muscle preparations are scarce in the scientific literature as of now.

***Objective:***

**I.** The first part of the present study was aimed at giving an up-to-date overview about ERS and testing the electrophysiological mechanisms underlying its lately described pharmacological responses including the suppressing effect of phosphodiesterase-3 (PDE-3) inhibitors and ajmaline.

**II.** The goal of the second part of the study was to investigate whether significant divergences in the APD-shortening effects of the two enantiomers of mexiletine exist, applied either alone or in combination with sotalol.

***Methods and Results:***

**I.** Transmembrane action potentials (AP) were simultaneously recorded from epicardial and endocardial regions of coronary-perfused canine ventricular wedge preparation, together with a transmural pseudo-ECG. The transient outward potassium currents ($I_{to}$) agonist NS5806 (7-15 μM) and the calcium current ($I_{Ca}$) blocker verapamil (2-3 uM) were used to induce an ERP and VT/VF. Following stable induction of arrhythmogenesis, the PDE-3 inhibitors cilostazol and milrinone or isoproterenol were added to the coronary perfusate. All were effective in restoring the AP dome in the left ventricular (LV) epicardium, thus

abolishing the repolarization defects responsible for phase 2 reentry (P2R) and arrhythmogenesis. Using voltage clamp techniques applied to canine LV epicardial myocytes, both cilostazol (10 μM) and milrinone (2.5 μM) were found to reduce $I_{to}$ by 44.4% and 40.4%, respectively, in addition to their known effects to augment $I_{Ca.}$

In another series of experiments we compared the effect of ajmaline on mild and accentuated ERS and BrS patterns. Brugada syndrome phenotype was mimicked by using the ATP-sensitive potassium current ($I_{K\text{-}ATP}$) agonist pinacidil (1-5 μM) and $I_{to}$ agonist NS5806 (7 μM) prior to the addition of ajmaline. In response to ajmaline infusion, J wave syndrome phenotypes with different grade of aggravation behaved bidirectionally depending on the size of AP notch and J wave the preparation displayed before the administration of ajmaline.

**II**. For analyzing the effects of mexiletine's levo- and dextrorotatory isomers, APs were recorded from isolated canine papillary muscle preparation, using conventional capillary glass microelectrode technique. Recordings were obtained in the absence and presence of R- and S-mexiletine alone, sotalol alone and sotalol combined with either R- or S-mexiletine. Significant differences in the effects of mexiletine's enantiomers on the studied electrophysiological parameters could not be observed.

***Conclusions:***

**I.** Our findings suggest that PDE-3 inhibitors exert an ameliorative effect in the setting of ERS by producing an inward shift in the balance of currents in the early phases of the epicardial AP via inhibition of $I_{to}$ as well as augmentation of $I_{Ca}$, thus reversing repolarization defects underlying the development of P2R and VT/VF. The ambiguous impact of ajmaline to suppress ERP but accentuate BrS pattern depends critically on the size of epicardial AP notch and consequent J wave.

**II.** Both optical isomers of mexiletine have similar effect on basic electrophysiologic parameters of canine papillary muscle, including their action to reverse sotalol-induced APD-prolongation. This significant re-abbreviating effect may also apply to other acquired long QT syndrome variants and explains racemic mexiletine's potency to control the related TdP tachyarrhythmias.

***Abbreviations:***

***AP***: transmembrane action potential
***APA***: amplitude of action potential
***APD***: action potential duration
***ATP***: adenosine-triphosphate
***BrS:*** Brugada syndrome
***cAMP***: cyclic adenosine-monophosphate
***CT***: conduction time
***ECG***: transmural electrocardiogram
***EG***: bipolar electrogram recorded from the epicardial (or endocardial) surface
***EDR***: epicardial dispersion of repolarization
***Endo***: endocardium/ endocardial
***Epi***: epicardium/epicardial
***ERP***: early repolarization pattern
***ERS***: early repolarization syndrome
$I_{Ca}$: L-type calcium current
$I_{K\text{-}ATP}$: ATP-sensitive potassium current
$I_{Na}$: cardiac voltage-gated fast sodium current
$I_{to}$: transient outward current
***IVF***: idiopathic ventricular fibrillation
***Jp***: peak of the J wave (or the onset of end-QRS slur)
***LV***: left ventricle
***MDP***: maximal diastolic potential
***P2R***: phase 2 reentry
***PDE-3***: phosphodiesterase-3
***PKA***: protein kinase A (cAMP-dependent protein kinase)
$V_{max}$: maximal upstroke velocity of phase 0
***VT***: polymorphic ventricular tachycardia
***RV***: right ventricle
**RVOT**: right ventricular outflow tract
***SCD***: sudden cardiac death
***TDR***: transmural dispersion of repolarization
***VF***: ventricular fibrillation

# I. INTRODUCTION

## I.1. Early repolarization syndrome and early repolarization pattern

### *I.1.1. Overview*

Early repolarization syndrome (ERS) is one of the main representatives of J wave syndromes, the unique group of electrical heart diseases characterized by the appearance of distinctive J waves in certain leads of the standard 12 lead ECG and increased vulnerability to malignant ventricular arrhythmias.

Although the early repolarization ECG-pattern (ERP) has been first described more than 90 years ago as an accompany of hypercalcaemia [Kraus 1920, Sridharan 1984] and hypothermia [Tomaszewski 1938; Osborn 1953, Phillipson 1967], it has drawn actual widespread attention of the scientific audience only in recent years, since its association with life-threatening arrhythmias including idiopathic ventricular fibrillation (IVF) has been suspected by experimental and later confirmed by several concurrent clinical studies [Yan 1996, Ant, Kalla 2000, Shu 2005, Letsas 2007, Haisaguerre 2008, Nam 2008, Rosso 2008, Tikkanen 2009, Derval 2011]. Thenceforth, the scientific literature in this field has shown an exponential expansion.

Why has it long been considered benign and why has its clinical impact remained hidden so long? One explanation is that the most malignant phenotype of ERP is rare and often displays a come-and-go nature, namely, it becomes accentuated mostly just directly before an arrhythmic event [Nam 2008, Aizawa 2012] – no wonder that its association with an increased arrhythmic risk has been recognized in the era of implantable recording devices. In this regard, it is also noteworthy that there is a significant discrepancy among studies when it comes to the definition of ERP [Patton 2016]: In the sense of earlier and some recent more permissive definitions, the pattern is so frequent in the general population that it is considered to be a benign normal variant of the ECG [Shipley 1936, Wasserburger 1961, Kambara 1976, Mehta 1995, Klatsky 2003, Maury 2013], and most individuals expressing an ERP are still at low risk for sudden arrhythmic death and remain lifelong asymptomatic. This leads us to the main challenge of the syndrome still to resolve: which ER-patients are vulnerable to sudden arrhythmic death and how to deal with those who are not.

*I.1.2. Diagnosis, classification and risk stratification*

As we discussed above, there is still a semantic confusion regarding the definition of early repolarization pattern. The term early repolarization was originally applied for J-point and ST segment elevation without a chest pain or apparent heart diseases and was thought to be a benign variation of the normal ECG [Shipley 1936; Wasserburger 1961, Kambara 1976]. Because the recent literature linked the increased arrhythmic risk to the presence of a J wave rather than ST elevation, the focus shifted to the J wave, so thus most experts active in this field consider ST elevation no more diagnostic for ERP. The definition and diagnostic criteria used in this thesis are based on the latest and most comprehensive expert consensus recommendations by Macfarlane et al and Antzelevitch et al. [Macfarlane 2015, Antzelevitch 2016]. Although some other studies challenge these approaches to the definition of ERP [Patton 2016], the aforementioned two are aimed at being more focused on the proarrhythmic aspects of ERP and ERS; therefore they are more likely to apply in the clinical practice, where the main challenge and absolute priority is to screen patients vulnerable to life-threatening ventricular arrhythmias.

*Early repolarization pattern (ERP)* is characterized by a distinct or slurred J wave at the terminal part (final 50% of the descending slope) of a prominent QRS complex, in other terms an end-QRS notch or slur, in at least two contiguous ECG-leads other than V1-V3. A distinct J wave has been proposed to be defined by its onset denoted as $J_o$, peak designated as $J_p$ and termination marked as $J_t$ (Figure 1/A). In case of slurred J wave/end-QRS slur, in which the onset of J wave is buried by the area under the QRS, its junction to the QRS is accounted as $J_p$ (Figure 1/B). The definitive diagnosis of ERP requires: $J_p \geq 0.1 mV$, QRS<120ms and the onset of the J wave ($J_o$ by distinct J wave and $J_p$ by slurred one) is above the zero-line. Although ST elevation is no more among the diagnostic criteria [Macfarlane 2015, Antzelevitch 2016], the course of the ST segment (ascending or horizontal/descending) is still informative in the classification and risk stratification of ERP/ERS (see below).

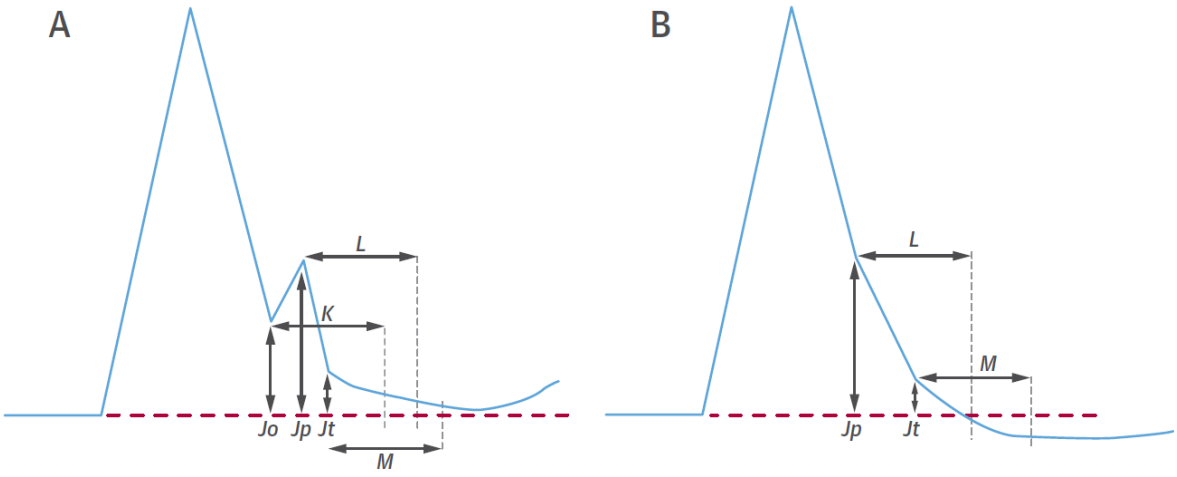


***Figure 1****:* Schematic illustration of notched (A) and slurred (B) J wave. $J_o$: onset of J wave, $J_p$: peak of the J wave, $J_t$: termination (end) of J wave, M: 100ms interval measured from $J_t$. J point elevation is to measure at $J_p$. The course of ST segment is to be defined at the M point (end of M interval). [Macfarlane 2015]

The conventional *classification* of early repolarization is based on the localization of the J waves and the course of the subsequent ST segments.

ST is considered *ascending* if it courses above $J_t$ when measured at 100ms after (M interval on Figure 1). Individuals displaying ERP with ascending ST segment, especially only in the lateral leads, are generally at low risk for VT/VF. It is a typical and frequent finding in young male athletes and is thought to be benign [Tikkanen 2011]. ST segment is to be evaluated as *horizontal/descending* when ST measured at the M interval tracks in line or below $J_t$ (Figure 1.) [Tikkanen 2011]. ERP with *horizontal/descending* ST segment is generally recognized as a more malignant pattern with an increased risk for VT/VF and cardiac mortality. [Tikkanen 2011, Rosso 2012, Rollin 2012]

ERP emerges in three typical line-ups on the standard 12-lead ECG: It is denoted as *Type I* if the pattern is displayed in *lateral* leads. Healthy individuals expressing *Type I* ERP are reportedly at lower risk for life-threating arrhythmias; moreover, many authors still account it as a benign ECG-variant when followed by an ascending ST segment [Patton 2016]. *Type II* indicates ERP manifesting in the *inferior/inferolateral* leads, whereas *Type III*, named also as *global ERP*, encompasses appearance of the pattern in multiple localizations including inferolateral + anterior and right ventricular leads. The latter one can fuel confusions to clear: If J waves appear exclusively in right ventricular (RV) leads, they are not diagnostic to ERP but Brugada syndrome. The diagnosis of Type III ERP requires inferior/inferolateral involment. Interestingly, global ERP is usually a temporary finding in

individuals with a basal inferolateral ERP, often only appearing at the time of arrhythmic episodes ("come-and-go"). In this sense, Type III can be considered as the more advanced phenotype of Type II. Patients displaying inferolateral or global early repolarization have higher risk for experiencing ventricular arrhythmias during their life. Global early repolarization is associated with the highest vulnerability to VT/VF including electrical storms [Tikkanen 2009, Rosso 2012, Rollin 2012].

Notwithstanding their presumably common electrophysiological basis, it is substantial to distinguish between *early repolarization pattern (ERP)* and *early repolarization syndrome (ERS)*. ERP is a relatively common finding in both physiologic and acquired conditions, such as athlete's heart, hypothermia, a long list of cardiac diseases, neurologic injury, electrolyte-imbalance, cocaine abuse, etc.; whereas ERS is considered to be a primary arrhythmia syndrome with much lower prevalence.

*Early repolarization syndrome (ERS)* is conventionally diagnosed when ERP coexists with documented aborted sudden cardiac death (SCD), ventricular fibrillation (VF) or polymorphic ventricular tachycardia (VT) with the exclusion of an organic heart disease. These traditional criteria have been refined and further specified by a newly proposed diagnostic score system, named Shanghai score system (Table 1), which pays regard also to the major risk factors for SCD associated with the syndrome, including J point elevation in the inferior leads, ERP with horizontal/descending ST segment, $J_p \geq 0.2$mV especially with T wave inversion, dynamic J wave/ST changes, clinical history of suspected or documented VT/VF and family history of SCD or ERP (Table 1.).[Antzelevitch 2016]

The pre- or coexistence of several other cardiac conditions with an early repolarization pattern have also been shown to predispose to sudden arrhythmic death or even increased all-cause mortality. These include Brugada- and short QT syndromes (or patterns), heart failure, hypothermia and ischemic heart diseases especially with newly emerging J wave.[Letsas 2008, Kawata 2013, Takagi 2013; Hasegawa 2016, Federman 2013, Bastiaenen 2010, Rudic 2012, Patel 2010, Patel 2012, Naruse 2012, Demidova 2014].

It has to be emphasized that the diagnostic criteria and risk stratification of both ERP and ERS have steadily been in progression, keeping up with the expanding clinical and experimental experience gathered in this field recently, and this evolution seems unlikely to stop at the current level. The recent consensus criteria should be approached as recommendations for the better comparability and risk assessment, and beyond doubt,

outcome-driven investigations should be directed to confirm or disprove their validity in the future.

| | Points |
|---|---|
| I. Clinical History | |
| A. Unexplained cardiac arrest, documented VF or polymorphic VT | 3 |
| B. Suspected arrhythmic syncope | 2 |
| C. Syncope of unclear mechanism/unclear etiology | 1 |
| **Only award points once for highest score within this category* | |
| II. Twelve-Lead ECG | |
| A. ER ≥0.2 mV in ≥2 inferior and/or lateral ECG leads with horizontal/descending ST segment | 2 |
| B. Dynamic changes in J-point elevation (≥0.1 mV) in ≥2 inferior and/or lateral ECG leads | 1.5 |
| C. ≥0.1 mV J-point elevation in at least 2 inferior and/or lateral ECG leads | 1 |
| **Only award points once for highest score within this category* | |
| III. Ambulatory ECG Monitoring | |
| A. Short-coupled PVCs with R on ascending limb or peak of T wave | 2 |
| IV. Family History | |
| A. Relative with definite ERS | 2 |
| B. ≥2 first-degree relatives with a II.A. ECG pattern | 2 |
| C. First-degree relative with a II.A. ECG pattern | 1 |
| D. Unexplained sudden cardiac death <45 years in a first- or second-degree relative | 0.5 |
| **Only award points once for highest score within this category* | |
| V. Genetic Test Result | |
| A. Probable pathogenic ERS susceptibility mutation | 0.5 |
| **Score (requires at least 1 ECG finding)** | |
| ≥5 points: Probable/definite ERS | |
| 3–4.5 points: Possible ERS | |
| <3 points: Nondiagnostic | |

ER = early repolarization; ERS = early repolarization syndrome; PVC = premature ventricular contraction; VF = ventricular fibrillation; VT = ventricular tachycardia.

***Table1****:* Shanghai score system for the diagnosis of early repolarization syndrome [from Antzelevitch 2016]

*I.1.3. Epidemiology*

An ERP is a relatively common electrographic finding, with a strong male predominance. Depending on anthropologic differences and the definition used for ERP, the prevalence ranges between 0.6% and 24% in the general population. $J_p$-elevation ≥ 0.2mV was reported in 0.3-0.64% of the general population. ERP is reportedly more prevalent in South-East Asia. Interestingly, ERP is more frequently observed among black and Australian aboriginal males but it is associated with lower arrhythmic risk in these anthropologic groups.

[Tikkanen 2009, Sinner 2010, Haruta 2011, Hayashi 2015, Perez 2012, Brosnan 2015]. VF/VT episodes occur mostly at increased vagal tone, during night or rest. Interestingly, the incidence of ventricular arrhythmias in the Japanese population has been reported to inversely correlate with air temperature, peaking in winter and early spring [Mizumaki 2012, Kim 2012, Maeda 2015, Shinohara 2016].

### *I.1.4. Cellular electrophysiology*

The pathophysiological background of the electrographic J waves has long been a matter of debate. The two main hypotheses are **repolarization** theory (1) and **depolarization** theory (2).

(1) In the sense of **repolarization** hypothesis, a net outward shift in the balance of currents active during the early phases of the cardiomyocyte's action potential (AP) leads to pronounced action potential notch in the ventricular epicardium but not in the endocardium (Figure 2 and 3), resulting in voltage gradient across the ventricular wall, which depicts on the ECG as J wave. A further accentuation of the action potential notch can lead to the highly proarrhythmic heterogeneous loss of the AP dome in the epicardium, giving rise to propagation of the second upstroke of the AP from sites where it is maintained to sites where it is lost(Figure 6). When this (concealed) phase 2 reentry (P2R) catches a vulnerable window opened up by increased dispersion of repolarization (lost AP domes), it can serve as trigger for premature ventricular complexes (PVCs) and VT/VF. [Yan 1996; Gussak 2000, Koncz 2013, Gurabi 2013]

(2) **Depolarization** hypothesis maintains that regional conduction delay is the cause underlying the electrographic manifestation of a J wave [Hoogendijk 2013, Meiborg 2016]. In this sense, ERP is considered to be a distinctly fragmented QRS complex, so thus J wave is actually an r' or R' wave [Huikuri 2015, Aizawa 2015].

Distinguishing between a J wave and an r' wave is not always possible with absolute confidence, but there exist tools and factors helping the distinction: J waves due to repolarization abnormality are likely augmented by pause and diminished by increased heart rate (Figures 2 and 3). Accordingly, ERS-patients usually suffer from arrhythmic episodes during rest, night or increased vagal tone [Mizumaki 2012, Kim 2012, Maeda 2015, Shinohara 2016]. On the contrary, QRS fragmentation usually aggravates by increased rate. A QRS fragmentation masquerading a J wave is unlikely to be an isolated finding in healthy

individuals. If the r' is present also in other leads but on the upslope or above the 50% of the QRS amplitude, especially in individuals present with organic heart disease, it is not definitive for ERP.

Although repolarization and depolarization abnormalities are certainly not mutually exclusive and their joint effect can be synergistic or potentiating, as of now only repolarization defect models are capable of recapitulating and explaining all features of the pattern and the syndrome, e.g. regional intracardiac differences [Koncz 2013], abnormally short activation–recovery intervals and marked dispersion of repolarization in the inferior and lateral regions of the LV [Ghosh 2010], response to changes in heart rate, quinidine, isoproterenol, hypothermia and increased vagal tone [Koncz 2013, Gurabi 2014, Patocskai 2016, Antzelevitch 2015]. Our research group pioneered in this work by publishing several studies using J wave syndrome models in the recent past [Koncz 2013, Gurabi 2014, Patocskai 2016 HR, Patocskai 2016 JACC-EP].

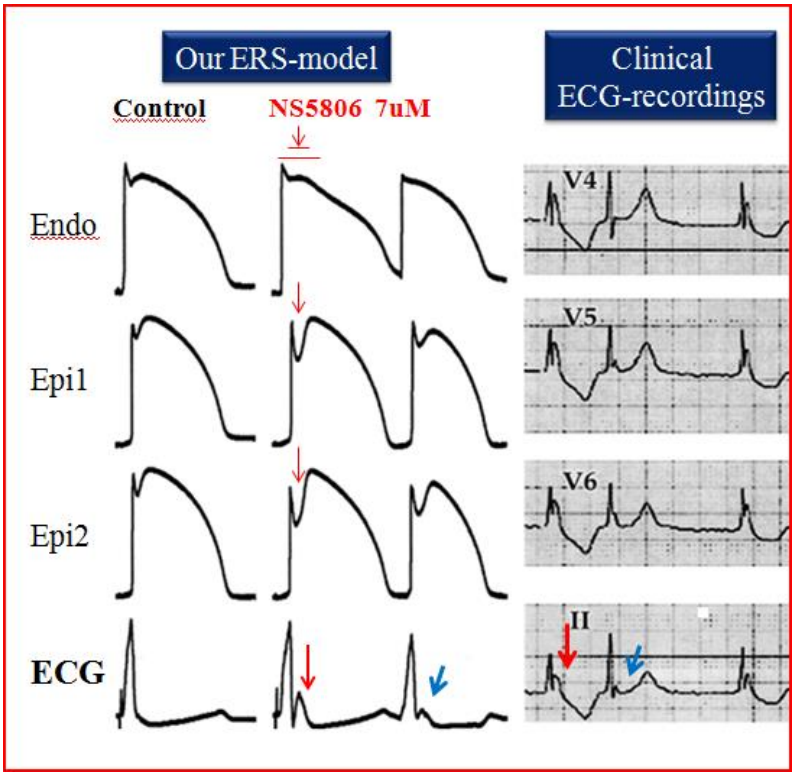


***Figure 2***: The pathophysiology and dynamics of J wave. **Left panel**: each column shows simultaneous action potentials recorded from one endocardial (Endo) and two epicardial sites (Epi) of canine left ventricular wedge preparation, together with a pseudo-ECG. Transmural voltage gradient depicts as J wave (red arrows), as a result of increased epicardial but not endocardial action potential notch (red arrows) under the application of $I_{to}$ agonist NS5806. An early premature beat caused J wave diminution (blue arrows), as a result of the reduced action potential notch secondary to the shortened RR interval. **Right panel**: Clinical ECG-

recordings of a patient with early repolarization syndrome. Similarly to our experimental setting, an early premature ventricular complex leads to a vast attenuation of J wave [Patocskai 2013, modified from Koncz 2013].

As discussed above, the corner stone of early repolarization syndrome is the transmural difference in the AP morphology across the ventricular myocardium, with special focus on the notch at phase 1, which is shaped by the balance of depolarizing and repolarizing early currents (Figure 3).

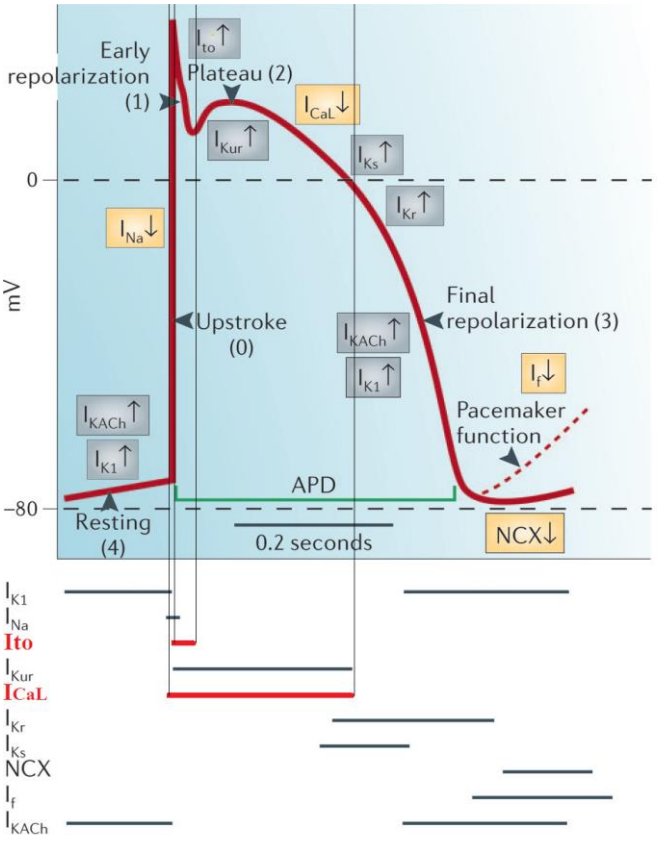


***Figure 3**:* Cardiac action potentials are shaped by the balance of inward and outward ion currents. Schematic, non-exhaustive epitome of the main ion currents of multiple cardiac cell types. [Modified from Nattel 2006]

Among these currents, under physiologic conditions, the transient outward potassium current ($I_{to}$) plays to most prominent role: A long list of experimental evidences demonstrates that augmenting the $I_{to}$ accentuates [Calloe 2009, Koncz 2013, Gurabi 2014], whereas blocking $I_{to}$ with 4-aminopyridine or quinidine abolishes the AP notch and J wave [Litovsky 1988, Yan 1996, Yan 1999, Koncz 2013, Gurabi 2014]. The magnitude of the AP notch closely follows the $I_{to}$ current density not just across the ventricular wall but also within the different regions

of the ventricles. Higher intrinsic level of $I_{to}$ current and consequently higher AP notch magnitude has been observed in epicardium vs. endocardium, apical vs. basal left ventricle (Figure 4-5), and right ventricle (especially outflow tract) vs. left ventricle [Litovsky 1988, DiDiego 1996; Szabo 2005, Szentandrassy 2005, Koncz 2013]. Interestingly, the higher $I_{to}$ current density correlates with higher expression of not the alpha channel subunits but an accessory subunit, KChIP2 (Figure 4C) [Rosati 2001; Rosati 2003; Zicha 2004, Gaborit 2007].

The higher $I_{to}$ density in the right ventricle and the apical left ventricle (Figures 4 and 5) explains why the global and inferior/inferolateral ERP implies more arrhythmic risk when compared to the lateral type. The channel kinetics of $I_{to}$, its relatively slow recovery from inactivation, is responsible for the inverse rate dependency and pause-dependent accentuation of epicardial AP notch and electrographic J wave [Koncz 2013, Huikuri 2015].

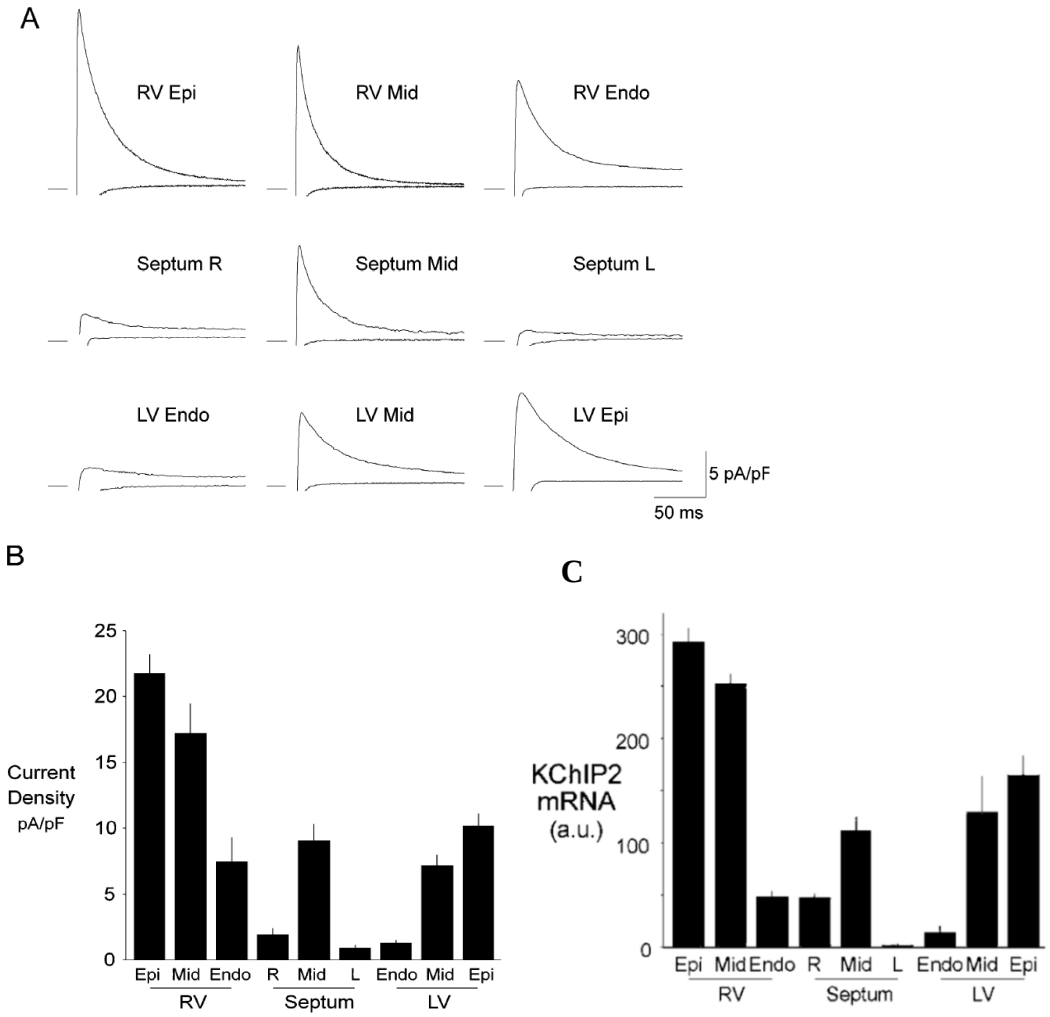


***Figure 4**:* Distribution of $I_{to}$ current and expression of KChIP2 mRNA in the canine ventricles [modified from Rosati 2003].

**A:** Representative $I_{to}$ current traces from various regions and layers of the canine ventricles. Current responses to steps from a holding potential of -70 mV to -20 mV (lower trace) and +50 mV (upper trace) are shown in each set of recordings. The sodium current was partially inactivated by a preceding 10 ms step to -45 mV at both traces.

**B:** Comparison of peak $I_{to}$ current densities (mean ± SEM) from each region and layer of the ventricles. Epi: epicardium, Mid: midmyocardium, Endo: endocardium, RV: right ventricle, LV: left ventricle, septum: interventricular septum.

**C:** KChIP2 mRNA expression (mean ± SEM) as determined by quantitation of RNAse protection gels using a PhosphorImager.

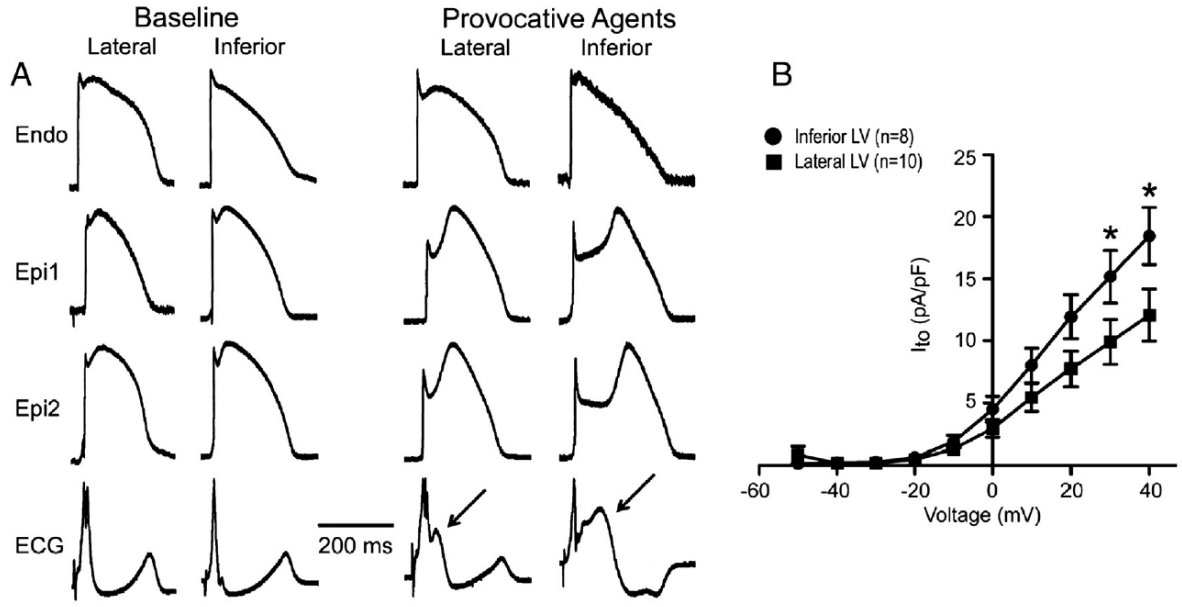


***Figure 5***: The inferior left ventricular (LV) epicardium expresses higher $I_{to}$ density and consequently higher action potential notch magnitude compared to the epicardium of the lateral wall, serving as the cellular basis for greater vulnerability of the inferior wall to early repolarization syndrome-associated arrhythmias. **A**: Simultaneous action potential and ECG recordings from canine LV wedge preparations isolated from the inferior and lateral regions of the same hearts. Groupings are identical as shown in Figure 2. First two column: under baseline conditions, second two column: under the administration of the provocative agents: a combination of NS5806 (7 μM) + verapamil (3 μM) + acetylcholine (ACh) (3 μM).

**B**: Current-voltage relation for $I_{to}$ density in inferior vs. lateral LV epicardial cardiomyocytes [modified from Koncz 2013].

$I_{to}$ current is strictly regulated by the vegetative system via the cAMP/PKA pathway [Gallego 2005]. The aggravating effect of increased vagal tone and the ameliorative impact of isoproterenol on ERP are attributed to their action to decrease or elevate the cardiomycyte's cAMP level, via activating muscarinic or adrenergic receptors, respectively. Our research group has recently demonstrated, in the setting of ERS, that acetylcholine (ACh) is capable of augmenting action potential notch and even triggering phase 2 reentrant arrhythmias; whereas isoproterenol exerts opposing effects [Koncz 2013]. However it should be noted that sympath(omim)ethic/ parasympath(omim)ethic effects and intracellular cAMP have an extremely broad-range impact on cellular functions including other membrane currents e.g. the L-type calcium-current ($I_{CaL}$).

Although $I_{to}$ is crucial, it is not the only contributor of forming the action potential notch. Loss of function or block of the cardiac fast sodium current ($I_{Na}$) has been shown to augment AP notch and J waves by numerous studies. However, in the absence of a prominent AP notch and $I_{to}$, loss of $I_{Na}$ in itself is incapable of producing any sign of J wave syndrome pattern (Figures 14-16) [Park 2015, Patocskai 2016 JACC-EP].

The other main depolarizing early current in ventricular cardiomyocytes is $I_{CaL}$. It plays the principal role in the creation of the 2$^{nd}$ upstroke and plateau-phase of an action potential with spike-and-dome morphology (Figure 3); therefore it is the ultimate "executor" of phase 2 reentry (P2R). One of the physiological roles for $I_{to}$ is thought to be to increase the electrochemical driving force for calcium ions, via counteracting the intracellular positive charge-load produced by the influx of sodium and calcium ions. At an extreme unfortunate constellation of co-factors, this counteraction can reach beyond the activation threshold of $I_{CaL}$, leading to all-or-none repolarization at the end of phase 1 (Figure 6). At this point, one cell loses its AP dome; meanwhile others produce an increased delay of the 2$^{nd}$ upstroke. P2R occurs when this maintained but delayed 2$^{nd}$ upstroke propagates to sites where it is lost (Figure 6). This AP-combination of maintained and lost domes can develop even without any baseline difference between the two cells. The development of an action potential can be best described mathematically as a diverse nonlinear dynamical system. At a certain balance of the co-factors, the behavior of this type of systems ("output") is often bistable, even in the absence of any alterations in intrinsic or extrinsic effectors ("input"). The dynamics of the development of all-or-none depolarization at the nadir of phase 1 of the AP is similar to the random and unpredictable development of early afterdepolarizations, action potential alternans and other AP-instabilities (beat-to-beat fluctuations) described by several in vivo and in silico studies [Bien 2006, Chialvo 1990, Karagueuzian 2013, Lerma 2007, Maoz 2009.

Maoz 2014, Sato 2010, Tran 2009, Watanabe 1995, Xie 2007] : At a certain point of the end of an accentuated-enough phase 1, either all-depolarization or none-depolarization has the same chance to develop as "output" of the system, without any difference in the "input" of the system. Ergo, even if the cells are completely identical to each other in every aspect, there is still a great chance that one will lose its action potential dome whereas the other one will turn into depolarization, purely due to the "dynamical chaos" (in its mathematical sense), as it has been described by studies modelling the development of P2R [Maoz 2009, Maoz 2014].

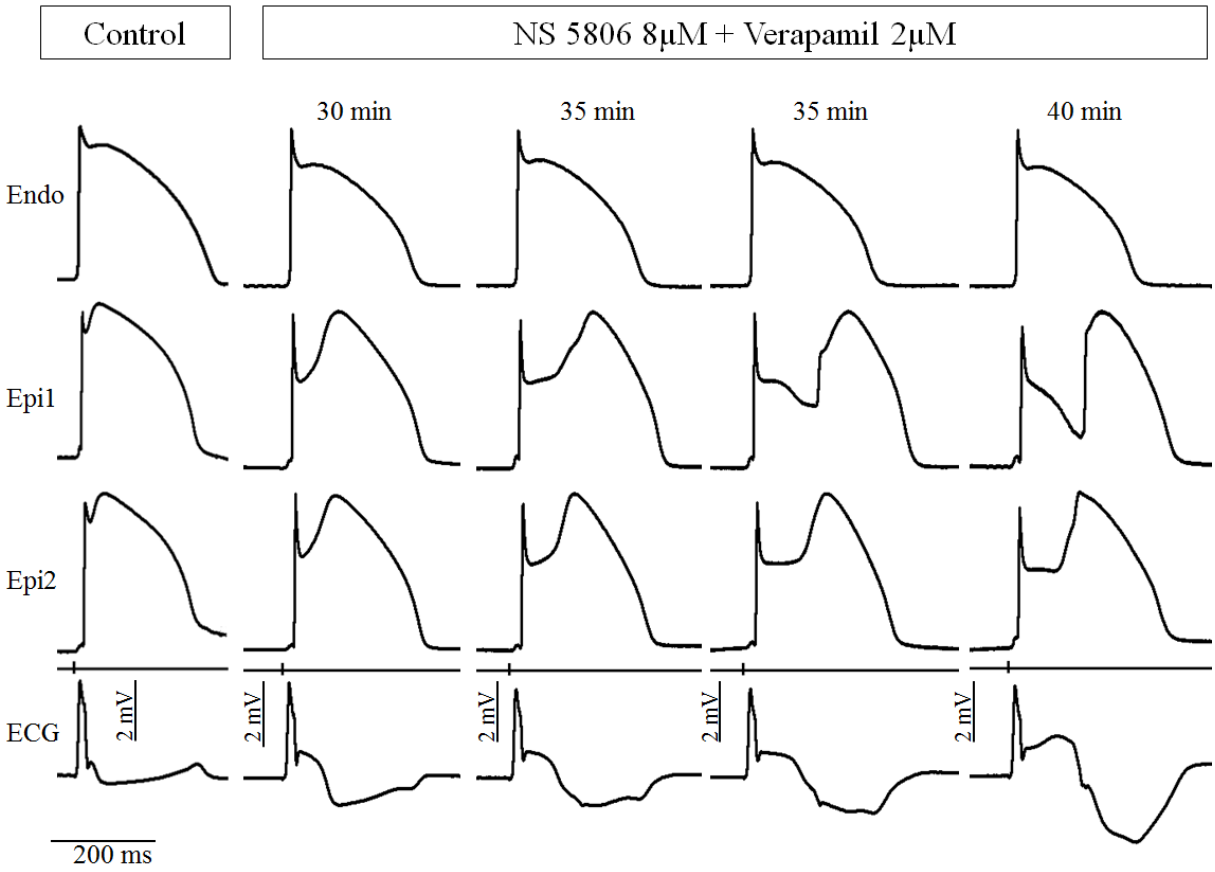


***Figure 6***: Development of phase 2 reentry in a canine ventricular model of J wave syndromes induced by the addition of $I_{to}$ agonist NS5806 and $I_{Ca}$ blocker verapamil to the coronary-perfusate. Traces are as shown in Figure 2. Extreme and heterogeneous accentuation of the epicardial but not endocardial action potential (AP) notch reaches beyond the level of all-or-none depolarization at the end of phase1, leading to loss of the AP dome and subsequent re-excitation at one site (Epi1) by propagation of the delayed second upstroke of the AP from a neighbor-site with maintained AP-dome (Epi2). [Patocskai and Antzelevitch 2014, unpublished data]

### *I.1.5. Genetic background*

Family members of patients suffering from ERS are more frequently affected by the syndrome than random individuals, and have an increased arrhythmic risk for SCD, suggesting a genetic background for the syndrome. The outward shift in the balance of currents, as the cellular basis for ERS, has been attributed to mutations in genes causing a gain of function in ATP-dependent potassium current ($I_{K\text{-}ATP}$) (*KCNJ8* and *ABCC9*) or $I_{to}$ [Hu 2014, Barajas-Martinez 2012, Haisaguerre 2009, Medeiros-Domingo 2010, Perrin 2014] or loss of function in $I_{CaL}$ (*CACNA1C, CACNB2* and *CACNA2D1*) [Burashnikov 2010, Napolitano 2011] or $I_{Na}$ (*SCN5A* and *SCN10A*) [Watanabe 2011, Hu 2014]. Gain of function mutations in $I_{to}$-coding or associated genes have been also linked to IVF and sudden unexplained death [Alders 2009, Guidicessi 2012]. Familial clustering of ERS has been reported with an autosomal dominant inheritance pattern with incomplete penetrance. Population-based studies have also suggested a degree of inheritance of ERP in the general population [Nosewothy 2011, Reinhard 2011] but the familial inheritance of malignant ER pattern is questionable [Haissaguerre 2008]. Taking into regard that many ERS-cases could not be linked to one well-defined ion channel mutation, a multigenetic/epigenetic predisposition for the syndrome is also reasonable to suggest ("extreme bad luck syndrome").

### *I.1.6. Current approaches to therapy and pharmacologic responses*

#### *Intracardiac (transluminal) implantable cardioverter defibrillator (ICD)*

ER**S** patients with survived sudden cardiac arrest or documented VF/VT episodes should receive an ICD (*Class I* recommendation). ICD has a *Class IIb* (may be considered) recommendation for individuals present with high-risk ER**P** plus a family history of sudden unexplained cardiac arrest, as well as for ER**P**-patients with syncope, seizures, or nocturnal agonal breathing plus family history of a definitive ER**S** (SCD or VT/VF) [Priori 2013].

The therapy of asymptomatic ER**P**-patients requires careful consideration. Although they have an increased risk for VT/VF compared to the general population (odds ratio ~ 3:1), the overall arrhythmia-incidence in these patients is still low; whereas the armamentarium of tools for risk stratification is quite limited at present. Taking into account also the high complication rate of transluminal implantation and chronic presence of intracardiac and intravessel electrodes, an ICD is not recommended (*Class III*) for asymptomatic individuals displaying an isolated ER**P** [Priori 2013].

A *completely subcutaneous ICD* offers a novel alternative therapeutic option for infants, young patients or patients with active lifestyle or with severe complications of implanted devices. Although its application in the other J wave syndrome sibling, Brugada syndrome, met with a warm response, long-term clinical experience or data regarding its application in ERS patients are lacking at present. [De Maria 2012, Griksaitis 2013, Rowley 2012, Bardy 2010]

*Pharmacologic responses and therapy*

ICD implantation is not an appropriate solution for infants and young children, or for low-risk patients, or for patients residing in regions of the world where an ICD is out of reach because of economic factors. The unique goal of a pharmacologic approach to therapy is to produce an inward shift in the balance of currents flowing during the early AP-phases of ventricular epicardium. No wonder that most of the conventional antiarrhythmics, like beta-blockers, verapamil, lidocaine/mexiletine and amiodarone are ineffective in supressing ERS-related VF/VT episodes either as acute or long-term therapy [Haisaguerre 2009].

In contrast, the adrenergic agonist **isoproterenol** has been found to be quite useful in reversing acute VT/VF and electrical storms, and **quinidine** –in its $I_{to}$-blocking concentration range– is effective in the long-term prevention of arrhythmic episodes and suppression of ERP [Nam 2008, Haisaguerre 2009, Aizawa 2013, Sacher 2014]. The cellular basis for their ameliorative effect has been described by our research team in a recent experimental study [Koncz 2013]: Both agents are capable of reducing dispersion of repolarization and abolishing P2R activity, via diminishing the AP notch and restoring AP dome (Figure 7) by their virtue of boosting $I_{Ca}$ (beta-adrenergic stimulation) and blocking $I_{to}$ current, respectively. According to the latest HRS/EHRA/APHRS guideline, isoproterenol have a Class IIa recommendation for the acute suppression of electrical storms. Quinidine received also a Class IIa designation for long-term prevention of arrhythmic episodes as adjuvant therapy to ICD. [Priori 2013]

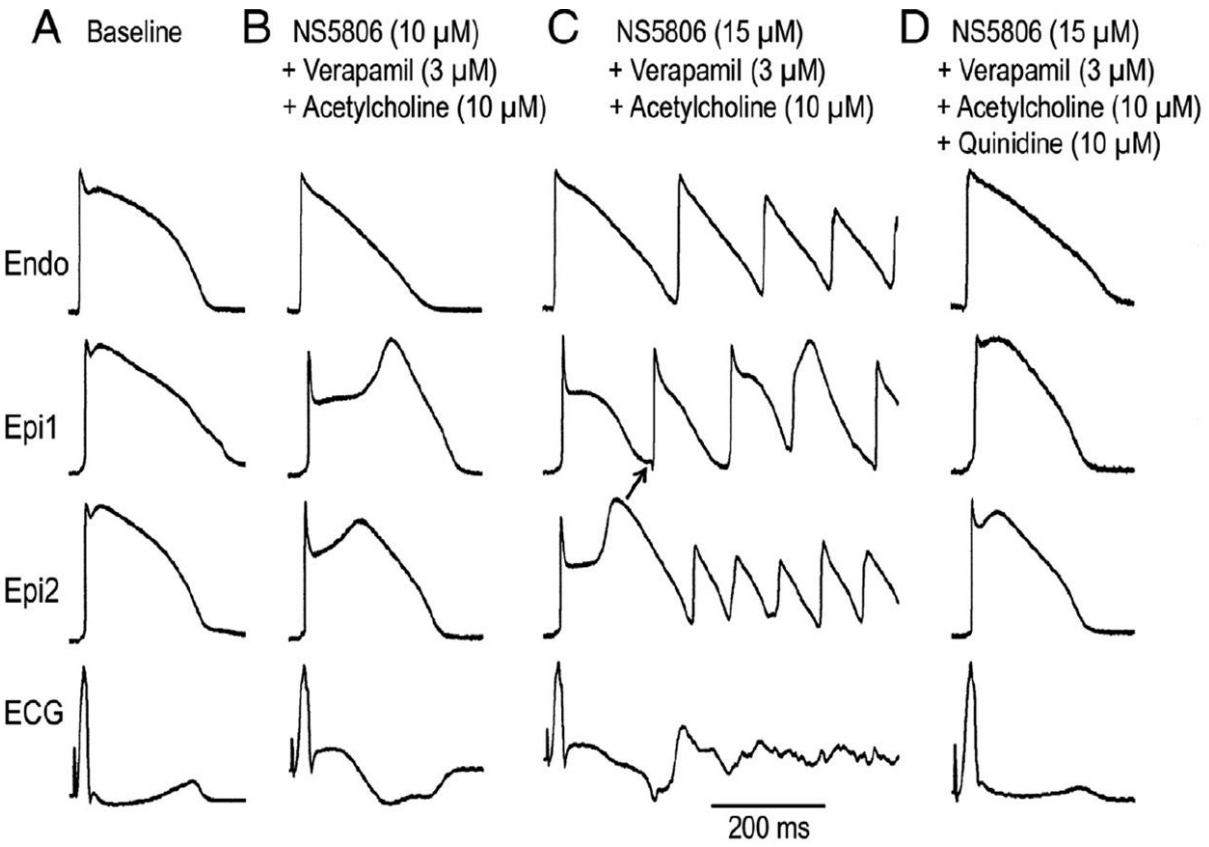


***Figure 7:*** Quinidine terminates VF via restoring normal AP morphology in a pharmacologic early repolarization model. Each column shows simultaneous action potentials recorded from the endocardium (Endo) and epicardium (Epi1 and Epi2) of arterially perfused canine left ventricular wedge preparation together with an ECG positioned along the transmural axis. Traces are grouped as in Figure 2. [modified from Koncz 2013]

For many patients neither isoproterenol nor quinidine offers an optimal long-term solution. Isoproterenol is a drug for acute use, and by (concealed) co-existence of other cardiac conditions, its application can be disadvantageous [Kondo 2015]. Quinidine seems to be beneficial only in a relatively high concentration, frequently accompanied by gastrointestinal side effects. Moreover, none of the compounds are 100% efficient, and both can facilitate other types of proarrhythmic activities in certain cases. Therefore, there is still a pressing need to find new, safe and effective pharmacologic therapeutic options. Recent clinical case reports demonstrated the efficacy of two novel candidates to control ERS-related VT/VF: The multi-channel blocker bepridil [Aizawa 2013, Shinohara 2014, Kaneko 2014] and the phospho-diesterase-3 (PDE3) inhibitor **Cilostazol**, or the combination of the two [Iguchi 2013, Shinohara 2014, Katsumi 2014].

ERS is not the only clinical entity embraced under the umbrella of the term J wave syndromes: Brugada syndrome (BrS) is also characterized by electrographic J waves (or ST

elevation), is associated with VT/VF and supposedly shares common cellular basis with ERS. Although overlap-phenotypes are also frequent, ERS mainly involves the LV, whilst BrS preferentially affects the right ventricular outflow tract (RVOT), so thus its ECG-sign is depicted in right precordial leads [Patocskai 2015, Antzelevitch 2016 CPC, Antzelevitch 2016 Springer]. Lately, clinical studies tested the effect of **ajmaline** on early repolarization pattern [Roten 2012, Bastiaenen 2013]. Ajmaline is originally a Class I/A sodium channel blocker, but it exerts multiple effects also on other ion-channels including $I_{to}$. The drug is in wide-spread clinical use to unmask Brugada syndrome, because it usually provokes or accentuates the isolated J wave/ ST-elevation in V1-V3 ECG-leads, the diagnostic ECG-pattern of the syndrome. It has also been observed that the compound aggravates (i.e. prolongs and splits) epicardial bipolar electrogram abnormalities [Sacher 2013]. Interestingly, the clinical works of Bastiaenen et al. [Bastiaenen 2013] and Roten et al. [Roten 2012] reported the opposite effect on early repolarization pattern: administration of ajmaline infusion **suppressed** the manifestation of mild ERP.

### *I.1.7. Goals of the study*

The first part of the present study was aimed at investigating the electrophysiological basis for the latest advances experienced in the field of ERS and ERP. Our principal aims were to (1) assess the cellular electrophysiological mechanisms underlying the antifibrillatory effects of **cilostazol** in ERS; (2) on this basis, test the applicability of a more potent PDE-3 inhibitor, **milrinone**; (3) compare their efficiency to the conventional choice of therapy, **isoproterenol**; (4) and to provide a direct test of the hypothesis that both PDE-3 inhibitors reduce $I_{to}$, significantly contributing to their ameliorative effect in J wave syndromes. (5) As an additional goal, our study is sought to resolve the controversy regarding **ajmaline**'s dissonant effect to augment or diminish the ECG pattern of J wave syndromes.

## I.2. Optical isomers of mexiletine and their co-administration with sotalol

**Mexiletine** is a Class I/B sodium channel blocker with similar cardiac actions to lidocaine but with good oral availability and longer half-life [Vaughan Williams 1998]. Its racemic form (containing both R-(-) and S-(+) enenatiomers) is in clinical use for the suppression of ventricular arrhythmias [Mason 1993, Singh 1990]. Racemic mexiletine use-dependently reduces the magnitude of fast sodium current [Hering 1983], decreases the

maximal velocity (slope) of phase-0 depolarization (Vmax) with a relatively fast onset and offset kinetics [Campbell 1983, Varró 1985], markedly slows premature conduction [Hohnloser 1982], suppresses abnormal automacity in Purkinje fibers [Sarkozy 2007] and shortens the durations of action potentials (APD) [Arita et al. 1979; Yamaguchi et al. 1979]. Lately, mexiletine has attracted attention afresh, due to its recently described potency to effectively terminate acquired long QT syndrome (LQTS)-related torsades de pointes (TdP) tachyarrhythmias [Badri 2015] and lately emerged application opportunities in the therapy of certain neurologic and myotonic disorders including neuropathic and chronic pain [O'Connor 2009, Park 2010], amyotrophic lateralsclerosis (ALS) [Weiss 2016], dystrophic and non-distrophic myotonia [Logigian 2010, Statland 2012] and Timothy syndrome [Gao 2013].

Mexiletine is reasonable to apply in combination with the drug sotalol, a beta-adrenergic receptor blocker that also possesses Class III antiarrhythmic effects by blocking the $I_{Kr}$ current and prolonging action potential duration (APD) and refractoriness. The combination of the two compounds has been reported to have an enhanced antiarrhythmic efficiency and less proarrhythmic side effects, especially TdP [Wagner 1987, Chézalviel Guilbert 1995, Ermakov 2014]. The benefits of this combination therapy have been attributed to the effect of mexiletine to counteract sotalol-induced APD-prolongation, early afterdepolarizations (EADs) and increased APD-range of premature action potentials [Varró 1990].

As mentioned above, mexiletine is administered as racemic compound. Although the differential effects of its stereoisomers on sodium current and excitability of skeletal muscle has been established more than twenty years ago [De Luca 1995], studies directed to exhaustive comparison of the electrophysiological effects of the R-(-) and S-(+) mexiletine isomers on cardiac ventricular muscle preparations were scarce until the recent past: In a lately published work of our research team we have investigated the electrophysiological effects of the levo- and dextrorotatory isomers of mexiletine in isolated **rabbit** cardiac muscle [Gurabi 2017]. We have observed a slower dissociation (offset) kinetics for R-(-) mexiletine from sodium channels than that for the S-(+) enantiomer.

The corresponding (second) part of the present study was directed to compare the effects of mexiletine's **R-(-)** and **S-(+) optical isomers** on the basic electrophysiological parameters of **canine** papillary muscle, with special focus on their effect either to shorten normal action potential duration or to re-abbreviate APD-prolongation of an acquired cause (i.e. $I_{Kr}$-block by sotalol), thus making an attempt to predict their consequential potency to reverse LQTS-related TdP tachyarrhythmias in a comparative manner.

II. METHODS

## II.1. J wave syndrome models

### *II.1.1. Coronary-perfused canine ventricular wedge preparation*

Our J wave syndrome models were created using coronary-perfused wedge preparation isolated from the hearts of adult mongrel dogs of either sex in conformance with the Guide for Care and Use of Laboratory Animals published by the National Institutes of Health (NIH publication No 85-23, Revised 1996) and approved by the Institutional Animal Care and Use Committee.

Wedge preparations for modelling ERS were excised from the free lateral and the free inferior wall of the LV and were perfused via distal branches of the left anterior descending coronary artery, left marginal artery or left posterior artery. For Brugada syndrome model, preparations were excised from the free anterior wall of the RV, and were perfused through the right marginal branch of the right coronary artery (RCA). The preparations were then placed in a tissue bath and perfused with oxygenated Tyrode's solution (mM): NaCl 129, KCl 4, NaH2PO4 0.9, NaHCO3 20, CaCl2 1.8, MgSO4 0.5, glucose 5.5, pH 7.4. The solution was bubbled with 95% O2 and 5% CO2, and maintained at 37±0.5°C. The perfusate was delivered using a peristaltic pump (Masterflex peristaltic pump, Cole Parmer Instrument Co, Niles, Illinois, USA) at a constant flow rate at 8-14 ml/min (1–2ml/min per gram of tissue). The preparations were equilibrated in the tissue bath until electrically stable, usually 1 hour, while stimulated at a basic cycle length of 1000 ms using bipolar silver electrodes insulated except at the tips, applied to the endocardial (Endo) surface.

A transmural ECG was recorded using two electrodes consisting of AgCl half cells placed in the tissue bath, 1.0 to 1.5 cm from the epicardial (Epi) and Endo surfaces of the preparation (Epi electrode is connected to the positive input of the ECG amplifier). Together with the ECG, transmembrane action potentials (AP) were simultaneously recorded from two epicardial (Epi 1 and Epi 2) and one endocardial site with the use of floating-glass microelectrodes (DC resistance = 10 to 20 MΩ) filled with 2.7 mol/l KCl, each connected to a high-input impedance amplifier. Impalements were obtained from the Epi and Endo surfaces of the preparation at positions approximating the transmural axis of the ECG recording. Spike 2 for Windows (Cambridge Electronic Design, Cambridge, England) was used to record and analyze the ECG and the AP. Together with the transmural ECG and AP recordings, bipolar

electrograms (EG) were recorded from the epicardial surface of the prepaprations. Bipolar surface electrograms were obtained using quadripolar electrophysiology catheters (St. Jude Medical Livewire™ 7F with 4 mm tip and 2-5-2 mm spacing), as well as Teflon-insulated (except at the tip) silver electrodes spaced 2 mm apart. Bipolar EG recordings were simultaneously band-pass filtered at 0.1-1000Hz, 10-1000Hz, 30-1000Hz and 10-250Hz, 30-250 Hz and 100-250 Hz to differentiate low and high frequency (slope) changes. In figures where the band-pass filter setting of the EG is not specified, the traces recorded with 0.1-1000Hz bandwidth are shown. The Epi and Endo surface of the preparation was mapped by using the transmembrane microelectrodes and the above mentioned electrophysiology catheter to reveal arrhythmic substrates.

*II.1.2. Pharmacologic models*

J wave syndromes were pharmacologically mimicked by targeting ion-channel currents affected by mutations associated with ERS and Brugada syndrome. In each model, the concentration of the mimicking compounds was increased until the stable induction of pronounced ERP or Brugada pattern, closely coupled premature ventricular complexes (PVCs), polymorphic tachycardia (VT) and/or fibrillation (VF).

*ERS model* was created using a combination of agents that inhibit inward (depolarizing) currents and that increase outward (repolarizing) currents: The model was designed to mimic a gain of function of the transient outward potassium current ($I_{to}$) using the $I_{to}$ agonist NS5806 (7-15 μM) and a loss of function of calcium channel current ($I_{Ca}$) using the $I_{Ca}$ blocker verapamil (2-3μM). Following stable induction of arrhythmogenesis, the PDE-3 inhibitors cilostazol and milrinone or isoproterenol were added to the coronary perfusate and then washed-out. In a second series of experiments, ajmaline alone was added to the coronary perfusate (without the previous administration of the provocative agents).

*A Brugada syndrome* model was designed to mimic a gain of function of the ATP-sensitive potassium current ($I_{K\text{-}ATP}$) using the $I_{K\text{-}ATP}$ agonist pinacidil (1-5 μM) and a loss of function of fast sodium channel current ($I_{Na}$) using the Class IA $I_{Na}$ blocker ajmaline (2-10 μM). A second Brugada syndrome model was created in order to compare the inducibility of preparations displaying small or pronounced AP notch, by applying ajmaline (10 μM) in the presence and absence of the $I_{to}$ agonist NS5806 (7 μM).

*II.1.3. Voltage-clamp measurement of $I_{to}$*

Cardiomyocytes were isolated from the epicardium of the canine left ventricle as described in details by Zygmunt et al. [Zygmunt 1997]. $I_{to}$ was measured at 36.5 ºC using the conventional whole-cell patch clamp techniques as specified by Hamill et al. [Hamill 1981]. $I_{to}$ was analyzed using series of 370 ms voltage steps ranged from -40 mV to +40 mV, each preceded by a 40 ms prepulse to -30 mV to discharge the sodium current. Holding potential was maintained at -80 mV. Series resistance was compensated at ~80% and cells with an Rs value greater than 5 MΩ were discarded from analysis. External solutions contained (in mM): 127 NaCl, 4 KCl, 10 HEPES, 1.8 CaCl2, 1.0 MgCl2, 10 glucose; pH=7.35 with NaOH. The pipette solution contained (in mM): 125 Potassium aspartate, 10 KCl, 10 NaCl, 1 MgCl2, 10 HEPES, 5 EGTA, 5 Mg2ATP; pH = 7.2 with KOH.

*II.1.4. Measurements and calculations*

The area of the epicardial action potential notch (Figure 8A) was quantified by notch-index (NI), calculated as the product of notch magnitude (NM) and notch duration ($t_{ph2}$-$t_{Ph0}$): *NI = NM x ($t_{ph2}$-$t_{ph0}$).* The epicardial NM was expressed as a percent of phase-0 amplitude: *NM = (phase 1 magnitude / phase 0 amplitude) x 100.* The epicardial AP notch duration was calculated as phase 0 to phase 2 interval ($t_{ph2}$-$t_{ph0}$), measured as the time-difference between the first two peaks of the 1st derivative of the AP: *Notch duration = $t_{ph2}$ - $t_{ph0}$.* The J wave area under the curve (AUC) was measured as illustrated in the ECG depicted in Figure 8A. The start of J-wave was defined using derivative of the ECG signal. In case of clear separation it was set at the time when this derivative is zero which corresponds to the notch between R wave and J wave. When this separation was not clearly visible, this time was set at the moment when the negative derivative attains its maximal value (i.e. minimal rate of decline) after the maximal downslope of the R wave. For a better basis of comparison, J wave area was normalized to R wave amplitude as follows: *J wave $AUC_r$ = J wave AUC/ R wave amplitude.*

Epicardial dispersion of repolarization (EDR) was calculated as the difference of the epicardial AP durations at 90% of repolarization ($APD_{90}$) in simultaneous recordings (Figure 8B). Activation time (AT) difference was accounted for as follows: *EDR = ($APD_{90Epi1}$ + $AT_{Epi1}$) – ($APD_{90Epi2}$ + $AT_{Epi2}$).* Transmural dispersion of repolarization (TDR) was calculated as the $APD_{90}$ difference of endocardial (Endo) and epicardial (Epi) action potentials simultaneously recorded (Figure 8B). Activation time differences were accounted for as follows: *TDR = ($APD_{90Endo}$ + $AT_{Endo}$) – ($APD_{90Epi}$ + $AT_{Epi}$).*

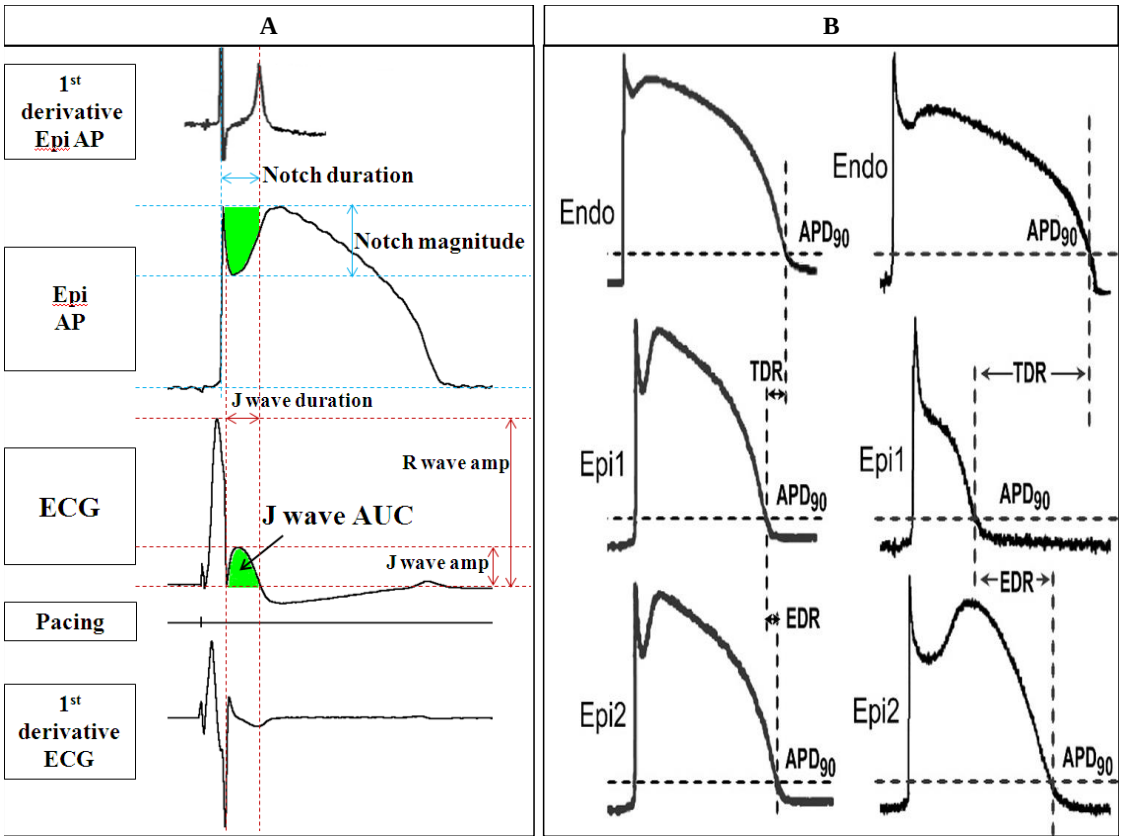


***Figure 8*:** Calculation of AP and ECG parameters. **A/ Top**: Quantification of the AP notch area. The AP notch index (NI) was calculated as the product of phase 0 to phase 2 interval ($t_{ph2} - t_{ph0}$) and notch magnitude (NM). NI = NM x ($t_{ph2} - t_{ph0}$) (see in the "Methods" section). **A/ Bottom**: Definition of J wave AUC with the assistance of 1st derivative of the ECG (see in the "Methods" section). **B:** Definition of epicardial dispersion of repolarization (EDR) and transmural dispersion of repolarization (TDR). [from Patocskai 2016 Heart Rhythm]

## II.2. Stereoisomers of mexiletine and their co-administration with sotalol

### *II.2.1. Isolated canine papillary muscle preparation*

Adult mongrel dogs were anaesthetized by using sodium pentobarbital (30 mg/kg) administered intravenously. After the hearts were removed through right lateral thoracotomy, the right papillary muscles were excised and immediately immersed into tissue bath and allowed to equilibrate for at least one hour, while superfused (flow rate 4–5 ml/min) with Locke's solution containing (in mM): NaCl 120, KCl 4, $CaCl_2$ 2, $MgCl_2$ 1, $NaHCO_3$ 22 and glucose 11. The solution was maintained at 37 °C and bubbled with 95% O2 and 5% $CO_2$, so thus its pH ranged between 7.40 and 7.45. During the equilibration period, the ventricular muscle tissues were stimulated at a basic cycle length of 1000 ms. Electrical pulses of 2 ms in

duration and twice diastolic threshold in intensity were delivered to the preparations through bipolar platinum electrodes. Transmembrane potentials were recorded with the use of glass capillary microelectrodes filled with 3 M KCl (tip resistance: 5 to 15 MΩ). The microelectrodes were coupled through an Ag–AgCl junction to the input of high impedance, capacitance-neutralizing amplifier (Experimetria 2004). Transmembrane AP recordings were processed by using APES software designed for instant (on-live) calculation and display of the following parameters: resting membrane potential, action potential amplitude, action potential duration at 10%, 25%, 50% and 90% repolarization and the maximum rate of rise of the action potential upstroke (Vmax). The preparations were stimulated with 1000 ms basic cycle length. After obtaining control measurements, the preparation was superfused either with 20 μM sotalol, or 20 μM R-(-)mexiletine or S-(+) mexiletine. In a second series of experiments, control recordings were followed by the combined application of sotalol and R- or S-mexiletine.

### II.3. Statistical analysis

Results are presented as mean ± S.E.M. Statistical analysis was performed using paired Student's *t*-test and one-way ANOVA for repeated measurements followed by pairwise comparisons corrected using the Holm-Sidak method, as appropriate. Statistical significance was considered at $p< 0.05$.

## III. RESULTS

### III.1 J wave syndromes

#### *III.1.1. Pharmacologic induction of early repolarization pattern*

ERP was induced by adding the transient outward potassium current ($I_{to}$) agonist NS5806 (7-15 μM) and the calcium channel blocker verapamil (2-3 μM) to the coronary perfusate, leading to accentuation of the action potential notch in epicardium but not endocardium. This heterogeneous accentuation resulted in augmentation of the electrocardiographic J wave secondary to amplification of the transmural voltage gradients (Figures 9-11). Increased concentrations of provocative agents caused a further increase of J wave area and notch-index (Figures 9-12; Table 2), leading to all-or-none repolarization at the end of phase 1 of the Epi AP (Figures 9-11). Loss of the Epi AP dome at some sites but not others resulted in a prominent increase in epicardial dispersion of repolarization (EDR) and

transmural dispersion of repolarization (TDR) (Figures 9-12; Table 2). The voltage gradient between the abbreviated Epi AP and the relatively normal Endo AP produced a prominent ST segment elevation (Figures 9-11). A prominent APD gradient developed between sites at which the dome was maintained and where the dome was lost, thus creating a vulnerable window within epicardium as well as between epicardium and endocardium across the left ventricular wall. Propagation of the AP dome from regions at which it was maintained to regions at which it was lost, caused local re-excitation via a P2R mechanism, leading to the development of closely coupled extrasystoles and polymorphic VT/VF (Figures 9-11).

Induction of ERP was observed in all experiments with. Table 2 and Figure 12 show the effect of the provocative agents to significantly increase notch-index, J wave area, EDR and TDR compared to the controls. PVT and/or VF developed in 26 of 28 LV wedge preparations, compared with 0 of 28 cases under control conditions.

| | **Notch-Index** | **EDR (ms)** | **TDR (ms)** | **J-w-AUC$_r$ (mV x ms)** | **Epi1 APD$_{90}$ (ms)** | **Epi2 APD$_{90}$ (ms)** | **Endo APD$_{90}$ (ms)** |
|---|---|---|---|---|---|---|---|
| ***Cilostazol*** | | | | | | | |
| Control | 199.07±44.9 | 16.2±8.2 | 17.8±4.3 | 4.3±2.0 | 203.6±7.8 | 182.8±5.6 | 217.7±5.1 |
| NS (7-15 μM) +Ver. (2-3μM) | 4863.6±669.4* | 137.9±8.1* | 111.8±13.4* | 56.6±12.2* | 252.2±7.8† | 109.4±5.6* | 237.2±14.3¶ |
| + Cilostazol (10μM) | 1041.7±124.2* | 11.9±3.8* | 21.3±3.8* | 15.0±4.0* | 218.4±7.5§ | 205.3±4.4* | 235.6±7.3¶ |
| Washout Cilostazol | 4809.8±590.7* | 123.3±10.6* | 106.9±11.2* | 53.0±6.2* | 252.7±10.1§ | 121.8±9.4* | 237.3±11.5¶ |
| ***Milrinone*** | | | | | | | |
| Control | 198.2±287 | 17.3±9.3 | 17.8±3.8 | 4.0±2.5 | 215.7±6.9 | 194.8±5.9 | 227.3±5.92 |
| NS (7-15 μM) +Ver. (2-3μM) | 4732.0±764.8* | 143.0±12.2* | 110±7.9* | 68.4±19.5* | 250.1±14.1§ | 104.9±8* | 230.1±4.7¶ |
| +Milrinone (2.5μM) | 1181.8±170.1* | 3.9±0.7* | 11.6±3.7* | 12.268±1.5* | 213.3±6.1¶ | 212.6±6.6* | 232.6±5.9¶ |
| Washout Milrinone | 4668.5±583.6* | 150.4±15.1* | 115.6±12.4* | 51.7±2.6† | 267.8±10.7† | 114.2±9.23* | 243.5±6.3¶ |
| ***Isoproterenol*** | | | | | | | |
| Control | 176.8±19.9 | 13.5±5.6 | 14.9±5 | 1.6±0.4 | 206.5±6.9 | 190.7±5.9 | 213.4±4.9 |
| NS (7-15 μM) +Ver. (2-3 μM) | 4114.7±400.8* | 123.9±11.9* | 88.9±5.2* | 46.0.0±4.9.* | 234.5±12¶ | 111.2±9.3* | 198.5±6.3¶ |
| +Iso. (1μM) | 406.9±65.6* | 5.9±1.6* | 13.6±4* | 7.8±2.7* | 164.1±8.3* | 158.6±7.7* | 179.±7.8¶ |
| Washout Iso | 3628.6.±795.9* | 87.7±25.4* | 67.1±15.0* | 39.5±8.2* | 207.9±22.6¶ | 116.0±14.3§ | 195.4±11.5¶ |

***Table 2*:** Effect of cilostazol, milrinone and isoproterenol on electrophysiological parameters in an experimental model of early repolarization syndrome. NS=NS5806; Ver.=Verapamil; Iso=Isoproterenol; J-w-$AUC_r$=J wave area (normalized). Data are presented as mean ± SEM**;** * p=<0.001; † p=<0.004; §: p<0.05; ¶ p>0.05. n=7 for cilostazol, n=6 for milrinone, n=7 for isoproterenol (Epi1 represents the longer, Epi2 the shorter epicardial $APD_{90}$).[from Patocskai 2016, HR]

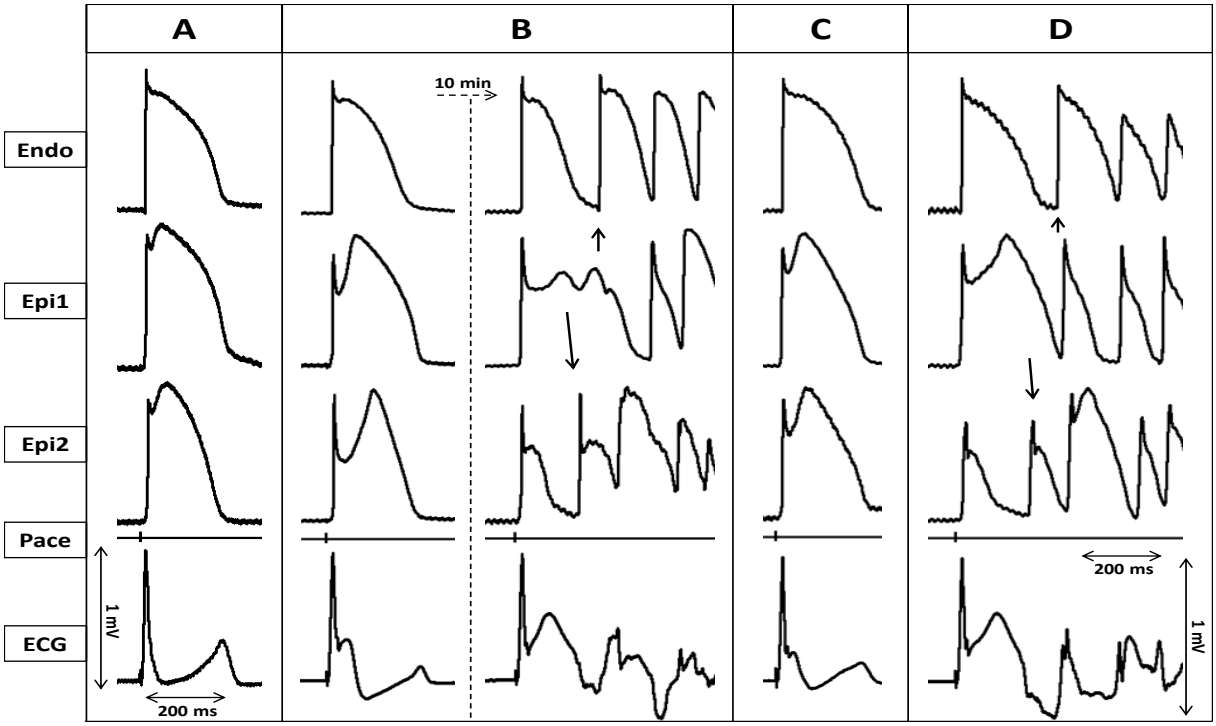


***Figure 9***: Ameliorative effect of **cilostazol** (10μM) in an arterially perfused canine left ventricular model of early repolarization syndrome. Each panel shows simultaneously recorded epicardial (Epi1, Epi2) and endocardial (Endo) action potentials, together with a pseudo-ECG. **A:** Control. **B:** Recorded 20 min and 30 min after addition of verapamil (2 μM) and NS5806 (7 μM) to the coronary perfusate. **C:** 15 minutes after addition of 10 μM **cilostazol** to the coronary perfusate. **D:** Recorded 15 min after withdrawal of cilostazol.
[from Patocskai 2016 Heart Rhythm]

*III.1.2. Ameliorative effects of cilostazol, milrinone and isoproterenol*

Addition of cilostazol (10 μM), milrinone (2.5 μM) or isoproterenol (0.1-1 μM) to the coronary perfusate restored the AP dome at all epicardial sites, reduced epicardial and transmural dispersion of repolarization, decreased J point and ST segment elevation and terminated all arrhythmic activity. Figures 9-11 show representative recordings of APs from LV wedge preparations obtained under baseline conditions, after NS5806 (7-15 μM), + verapamil (2-3 μM), + PDE-3 inhibitor (10 μM cilostazol or 2.5 μM milrinone) or the sympathomimetic agent isoproterenol (0.1-1 μM) and after washout of the therapeutic compounds.

The effects of milrinone, cilostazol and isoproterenol on epicardial AP notch index, J wave area, EDR and TDR as well as $APD_{90}$ values for Epi1, Epi2 and Endo are summarized in Figures 12 and Table 2. All three agents, by virtue of their action to produce an inward shift of balance of currents, reversed the effect of the provocative agents, restoring all electrophysiologic parameters towards normal. Cilostazol (10 μM), milrinone (2.5 μM) and isoproterenol (0.1-1 μM) restored the AP dome at all epicardial sites, thus reducing notch index, J wave area, as well as epicardial and transmural dispersion of repolarization (Figures 9-12 and Table 2).

Figures 9-12 illustrate the development of polymorphic VT following exposure to NS5806 and verapamil and the effect of cilostazol (10 μM), milrinone (2.5 μM) and isoproterenol (0.2 μM) to normalize the ECG and to terminate all arrhythmic activity. Cilostazol (10 μM) abolished VT/VF in 7 of 8 preparations, whereas milrinone (2.5 μM) abolished VT/VF in 6 out of 7 preparations, and isoproterenol terminated VT/VF in 7 of 8. In all cases, washout of the drug resulted in reappearance of arrhythmic activity (Figures 9-11).

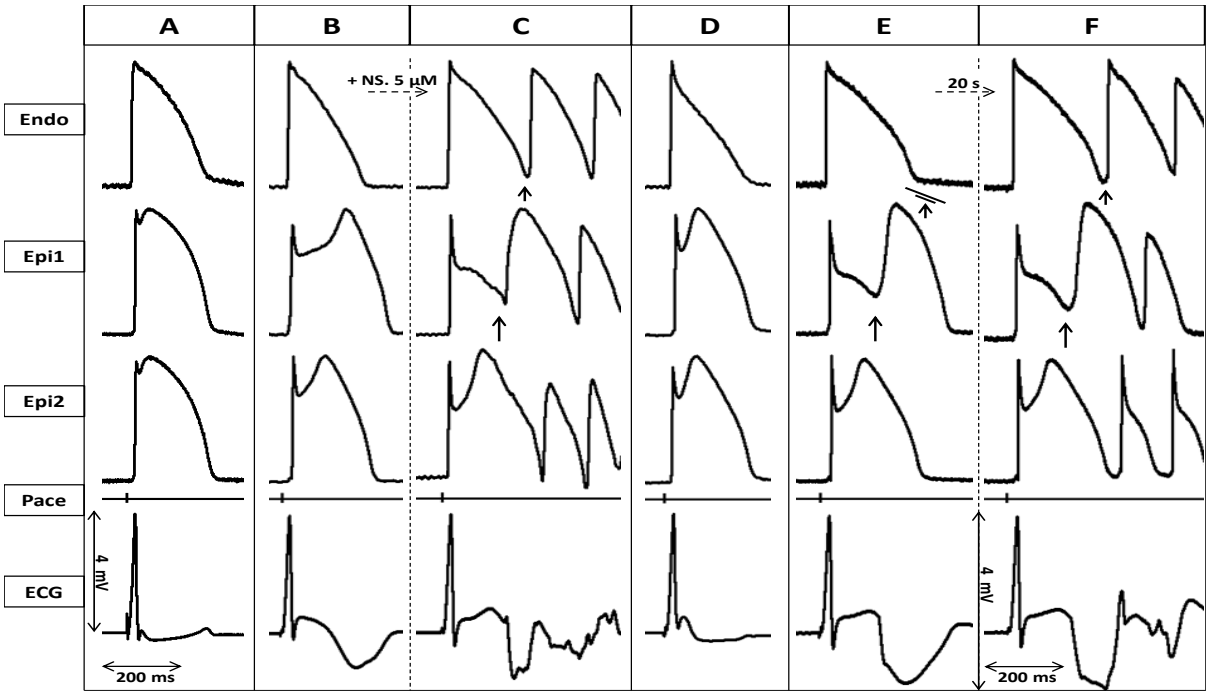


***Figure 10*:** Ameliorative effect of **milrinone** (2.5μM) in an arterially perfused canine left ventricular model of early repolarization syndrome. Each panel shows simultaneously recorded epicardial (Epi1, Epi2) and endocardial (Endo) action potentials, together with a pseudo-ECG. **A:** Control. **B:** Traces recorded 40 min after the addition of $Ca^{2+}$-channel blocker verapamil (2μM) and $I_{to}$-agonist NS5806 (7 μM). **C:** 15 minutes after raising NS5806 concentration to 12 μM. **D:** 10 minutes after addition of **milrinone** 2.5μM to the coronary perfusate. **E:** 20 minutes after the discontinuation of milrinone infusion. **F:** 20 seconds later. [from Patocskai 2016 Heart Rhythm]

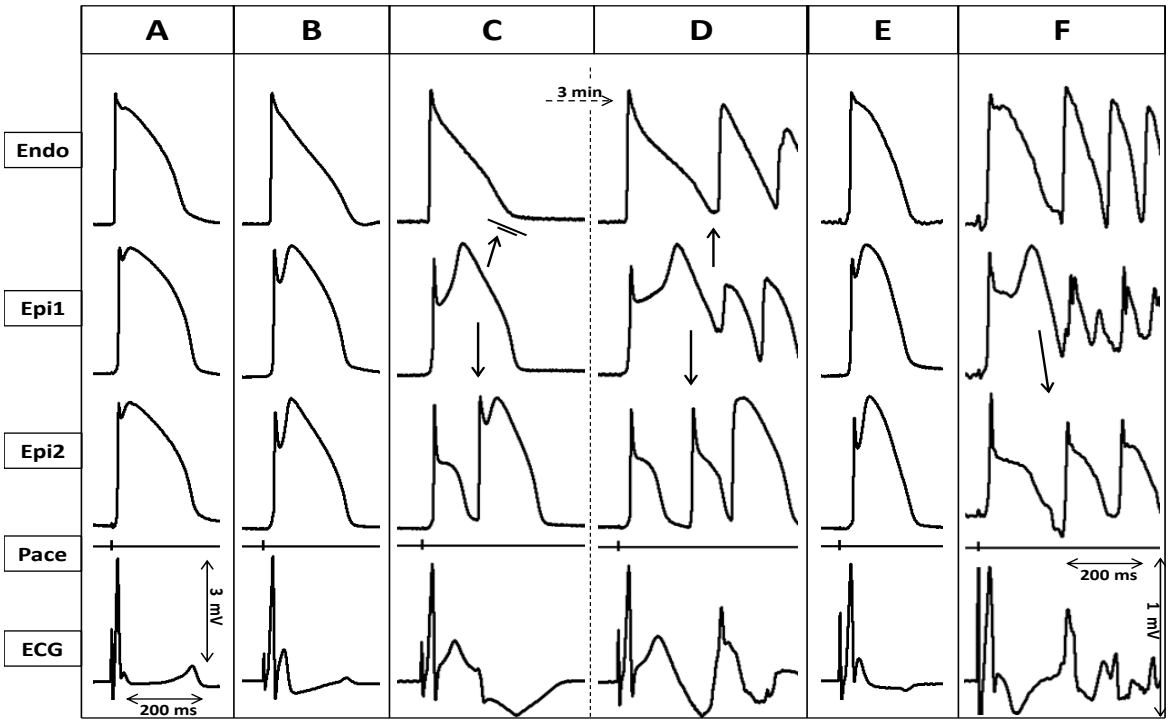

***Figure 11*:** Ameliorative effects of **isoproterenol** (0.2 μM) in an arterially perfused canine left ventricular model of early repolarization syndrome. Simultaneously recorded epicardial (Epi1, Epi2) and endocardial (Endo) action potentials, together with pseudo-ECG positioned in the transmural axis. **A**: Control. **B**: 20 min after addition of the $I_{to}$ agonist NS5806 (12μM) to the coronary perfusate. **C**: After 16 min exposure time of verapamil (2μM), in addition to NS5806 (12μM).**D**: 3 minutes later. **E**: 5 min after the start of **isoproterenol (0.2μM)** infusion. **F:** 5 min after the discontinuation of isoproterenol infusion. [from Patocskai 2016 Heart Rhythm]

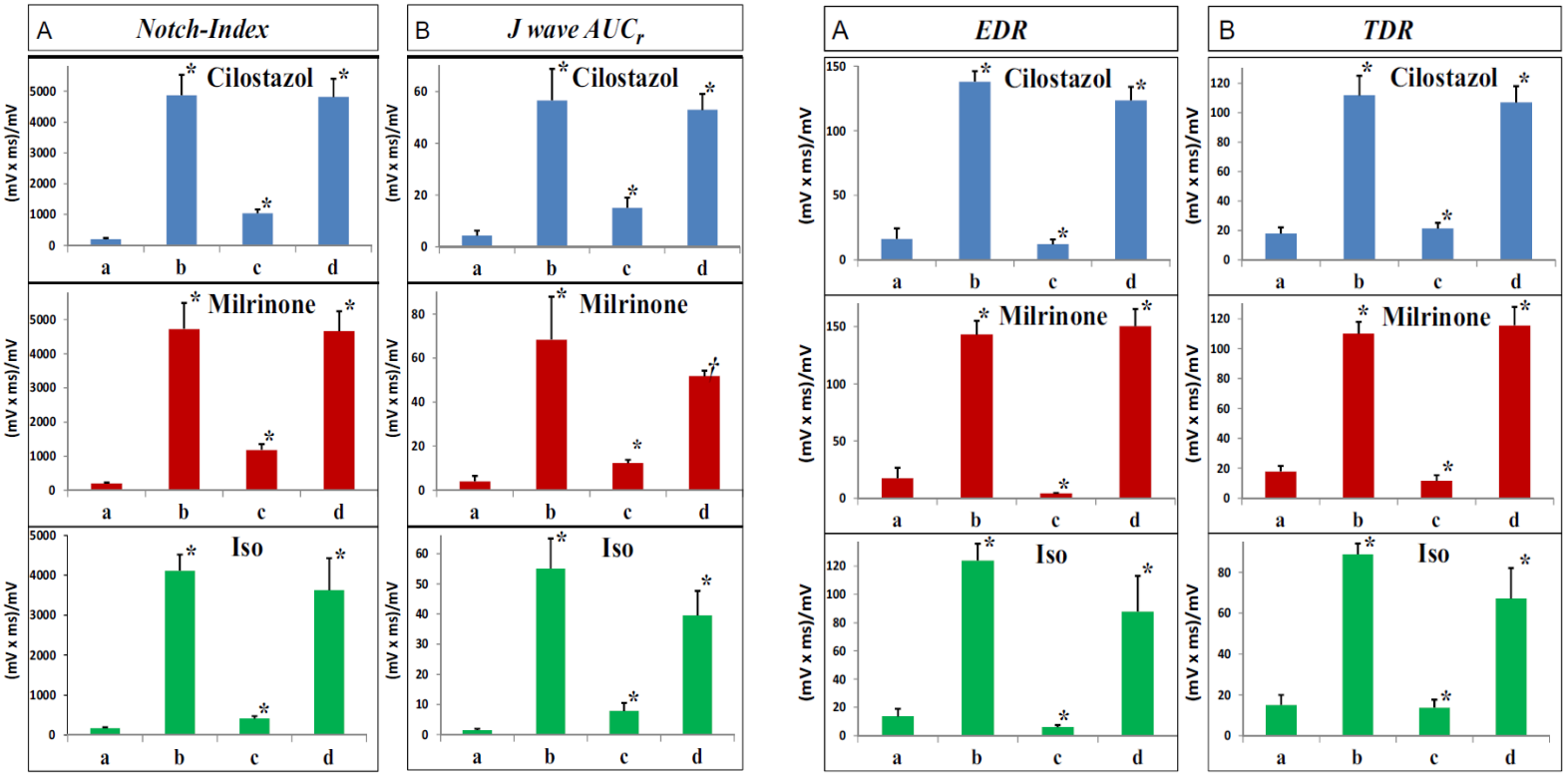


***Figure 12*:** Electrophysiological effect of cilostazol, milrinone and isoproterenol on early repolarization model. **Left panels:** Notch-index (left) and normalized J wave area (right) at each experimental step. In each panel: **a**. Control; **b**. Recorded after application of the $I_{to}$ agonist NS5806 and $I_{Ca}$ antagonist verapamil; **c**. Recorded after addition of cilostazol 10μM (top row), milrinone 2.5μM (middle row), or isoproterenol 1μM (bottom row); **d**. Recorded after wash-out of drugs. Data are presented as mean ± SEM. Significance is shown relative to previous experimental step: * p=<0.001; †p=<0.004. (n = 7 for cilostazol; n = 6 for milrinone; n = 7 for isoproterenol). **Right panels:** Epicardial (**EDR**, left) and transmural (**TDR**, right) dispersion of repolarization at each experimental step. In each panel: **a**. Control; **b**. Recorded after application of the $I_{to}$ agonist NS5806 and $I_{Ca}$ antagonist verapamil; **c**.

Recorded after addition of cilostazol 10μM (top row), milrinone 2.5μM (middle row), or isoproterenol 1μM (bottom row); **d**. Recorded after wash-out of drugs. Data are presented as mean ± SEM. Significance is shown relative to previous experimental step: * p=<0.001 (n = 7 for cilostazol; n = 6 for milrinone; n = 7 for isoproterenol). [from Patocskai 2016 Heart Rhythm]

*III.1.3. Effect of cilostazol and milrinone to reduce $I_{to}$*

The next step in our study was the evaluation of the effect of cilostazol and milrinone on transient outward potassium current of canine left ventricular epicardial myocytes using whole cell patch clamp techniques. Both PDE3 inhibitors led to a markedly reduced macroscopic $I_{to}$ current, contributing to their ameliorative effect in J wave syndrome models. It should be noted that milrinone exerted a similar reduction in peak $I_{to}$ current density to cilostazol, but already in a much lower concentration.

Results are shown in Figure 13. Left block represents the effect of cilostazol (10 μM), right block shows the effect of milrinone (2.5 μM). On each block, panels "A" show representative macroscopic $I_{to}$ traces recorded under control conditions and reduction of the current after addition of cilostazol (10 μM) or milrinone (2.5 μM). Peak $I_{to}$ was evaluated using a square depolarization pulse from -40 mV to +40 mV applied once every 5 seconds. Panels "B" represent the effect of cilostazol (10 μM) and milrinone (2.5 μM) on the current-voltage (I-V) relationship. Panels "C" show the normalized $I_{to}$ current density at +20 mV and +40 mV in control condition and after the addition of cilostazol or milrinone. At +40 mV, cilostazol (10 μM) reduced $I_{to}$ by 44.4 % (n=6, p<0.02), whereas milrinone (2.5 μM) reduced $I_{to}$ by 40.4 % (n=8, p<0.02).

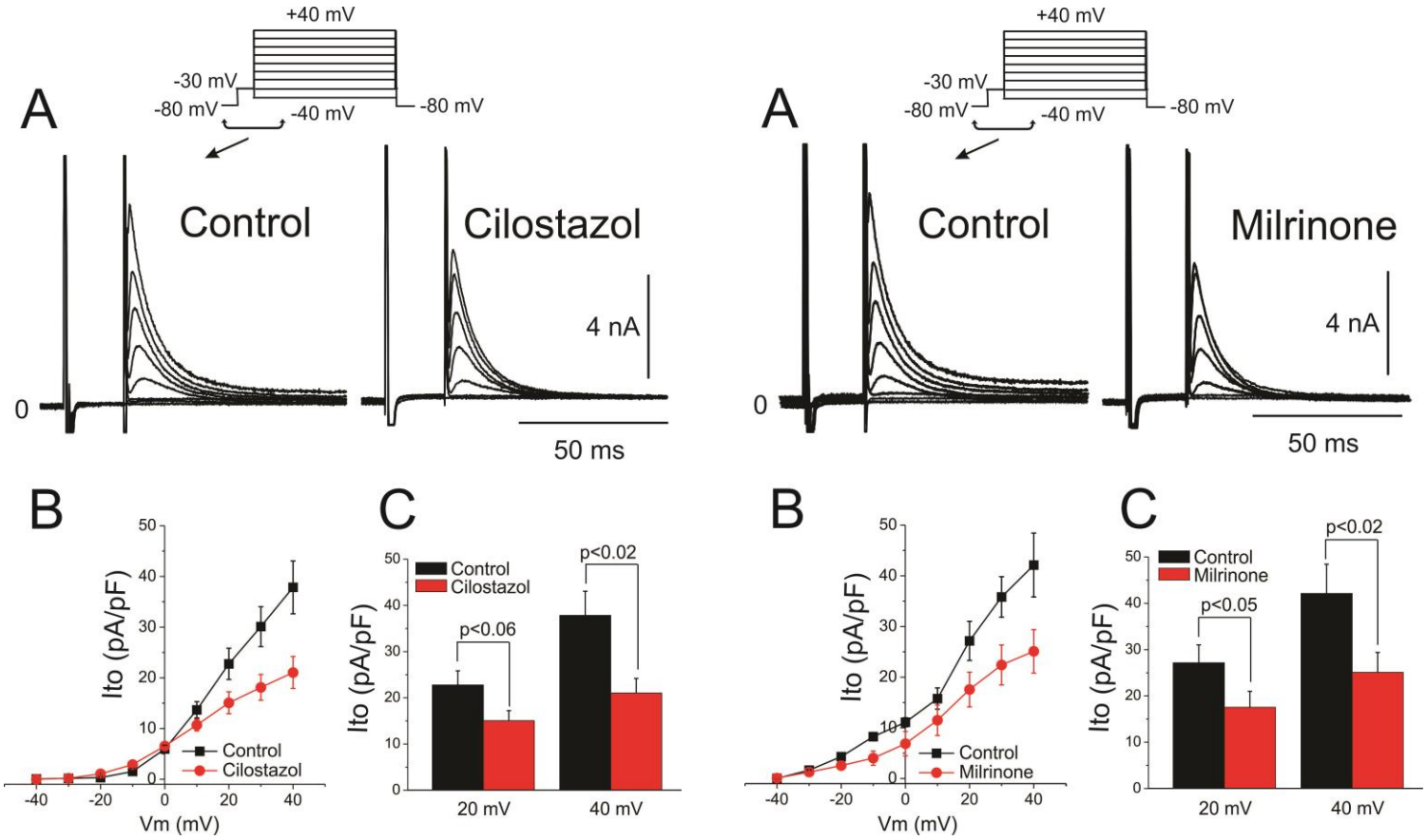


***Figure 13***: PDE3 inhibitors reduce the transient outward potassium current ($I_{to}$).

**Left block**: effect of cilostazol (10 µM). **Right block**: effect of milrinone (2.5 µM).

On both blocks: **A:** Representative macroscopic $I_{to}$ current traces for control and cilostazol (10 µM) or milrinone (2.5 µM). **B**. Current-voltage (I-V) relationship for normalized $I_{to}$ density in control and in response to 10 µM cilostazol (n=6 for each) or 2.5 µM milrinone (n=8 for each). **C.** Bar diagram showing $I_{to}$ (mean ± SEM) following a step to +20 and +40 mV in presence (red bars) and absence (black bars) of cilostazol or milrinone. Results are shown as mean ± SEM. [from Patocskai 2016 Heart Rhythm]

*III.1.4. Bidirectional effects of ajmaline on J wave syndrome pattern*

The size of baseline AP notch and J wave showed a relative high variability in our preparations (e.g. apical vs. basal LV and RV vs. LV), providing us a great opportunity to diversify the behavior of J waves in response to ajmaline depending on the intrinsic level of the tissue's AP notch. In preparations displaying small basal AP notch (Figures 14B and 15), ajmaline decreased the area of J wave and AP notch, presumably due to the multiple effects on various ion currents including $I_{to}$, as well as widening of the QRS, thus engulfing the J wave. These observations are consistent with clinical studies reporting improvement in the

ECG manifestation of early repolarization pattern following ajmaline-infusion [Bastiaenen 2013, Roten 2012]. For quantifying this association we compared the AP notch and J wave area of "inducible" and "non-inducible" cases of Brugada model experiments. Preparations that failed to develop the Brugada pattern (BrP) and arrhythmic activity ("non-inducible"), either spontaneously or in response to PES, displayed significantly lower J wave and AP notch area at baseline and after the addition of the provocative agents, than those in which the provocative agents were successful in inducing the ECG and arrhythmic manifestations of BrS ("inducible") (Fig. 14A). At baseline, inducible vs. non-inducible values were 4.5±1.1 vs. 1.1±0.2 ($p=0.0238$) for J wave area, and were 9.4±1.5 vs. 2.4±0.3 ($p=0.002$) for AP notch area (Figure 14C-D).

To confirm these findings, we compared the effect of high dose ajmaline (10μM) in the absence and presence of the $I_{to}$ agonist NS5806, in the same preparations. The results supported our conclusion that the effect of ajmaline is dependent on the magnitude of AP notch prior to introduction of ajmaline. This also provides an explanation for the RVOT-predominance of Brugada syndrome since this region of the heart displays the most prominent AP notch. As illustrated in Figure 15 and 16B, ajmaline (10μM), when applied alone, slightly reduced the size of the J wave and AP notch. Ajmaline, in this setting, produced a mild effect on the ST segment and epicardial electrogram despite prolongation of QRS and slowing of transmural conduction (Figure 16B). The effect was reversible upon washout (Figure 16C). When the epicardial AP notch was accentuated by pre-treatment with the $I_{to}$ agonist NS 5806 (7 μM) (Figure 16D), addition of ajmaline (10μM) led to marked accentuation of Epi AP notch, leading to the development of abnormal electrogram activity, Type I ST-elevation and concealed P2R. The appearance of abnormal electrogram activity was secondary to the inhomogeneous accentuation of the AP notch, loss of the AP dome and P2R (Figure 16E-F). This association was further supported by the observation that at the maximal effect of high-dose ajmaline, loss of the epicardial AP dome throughout the entire epicardium and subepicardium resulted in loss of the fractionated EG activity, despite the further prolongation of QRS and further slowing of transmural conduction (Figure 16G).

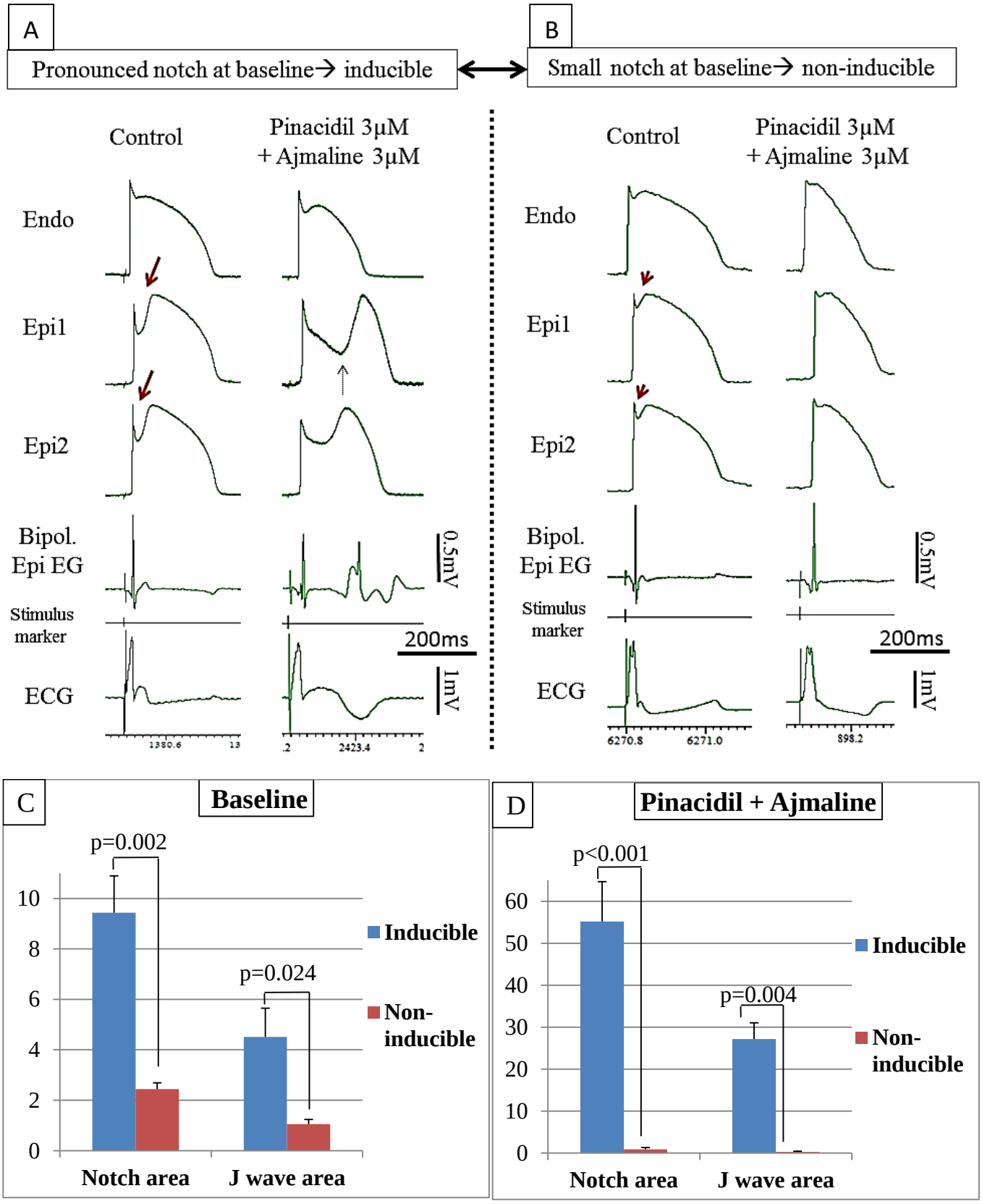


***Figure 14***: Inducibilty of aggravated J wave and phase 2 reentry depends on the magnitude of the epicardial action potential notch and consequentional J wave at baseline. Pharmacologic model of pinacidil + ajmaline in arterially perfused ventricular wedge praparation. **Panels A and B:** Each column shows action potentials (AP) simultaneously recorded from an

endocardial (Endo) and 2 epicardial (Epi1 and Epi2) sites together with a bipolar epicardial electrogram (Bipol. Epi EG) and an ECG recorded accross the bath. **A:** Preparation exhibiting a large spike and dome action potential morphology at baseline (control). The provocative agents induce a BrS ECG and concealed phase 2 reentrry giving rise to distinct late potentials (Bipol. Epi EG). **B:** Preparation exhibiting a relatively small spike and dome action potential morphology at baseline. The provocative agents do not induce a BrS ECG, but diminish the J wave. **Panels C and D:** Comparison of epicardial AP notch $area_r$ and J wave $area_r$ of preparations vulnerable (inducible) and non-vulnerable (non-inducible) to the induction of BrS pattern and arrhythmias. n=6 for inducible and n=5 for non-inducible preparations. **C**: Parameters at baseline. Inducible preparations showed an avarege 3.9 fold higher AP notch and 4.3 fold higher J wave area at baseline, compared to the non-inducible ones (inducible vs noninducible: p=0.002 and p=0.024 for notch $area_r$ and J wave $area_r$, respectively). **D:** After the addition of provocative agents, inducible preparations showed a pronounced **increase** (p=0.004 vs baseline), whereas non-inducible peparations showed a significant **decrease** (p=0.017 vs baseline) in both J wave and AP notch area. The provocative agents produced an avarage 60.5 fold higher notch area and 88.7 fold higher J wave area in inducible compared to non-inducible preparations (inducible vs. non-inducible: p<0.001 and p=0.004 for notch area and J wave $area_r$, respectively).[from Patocskai 2016, JACC-EP]

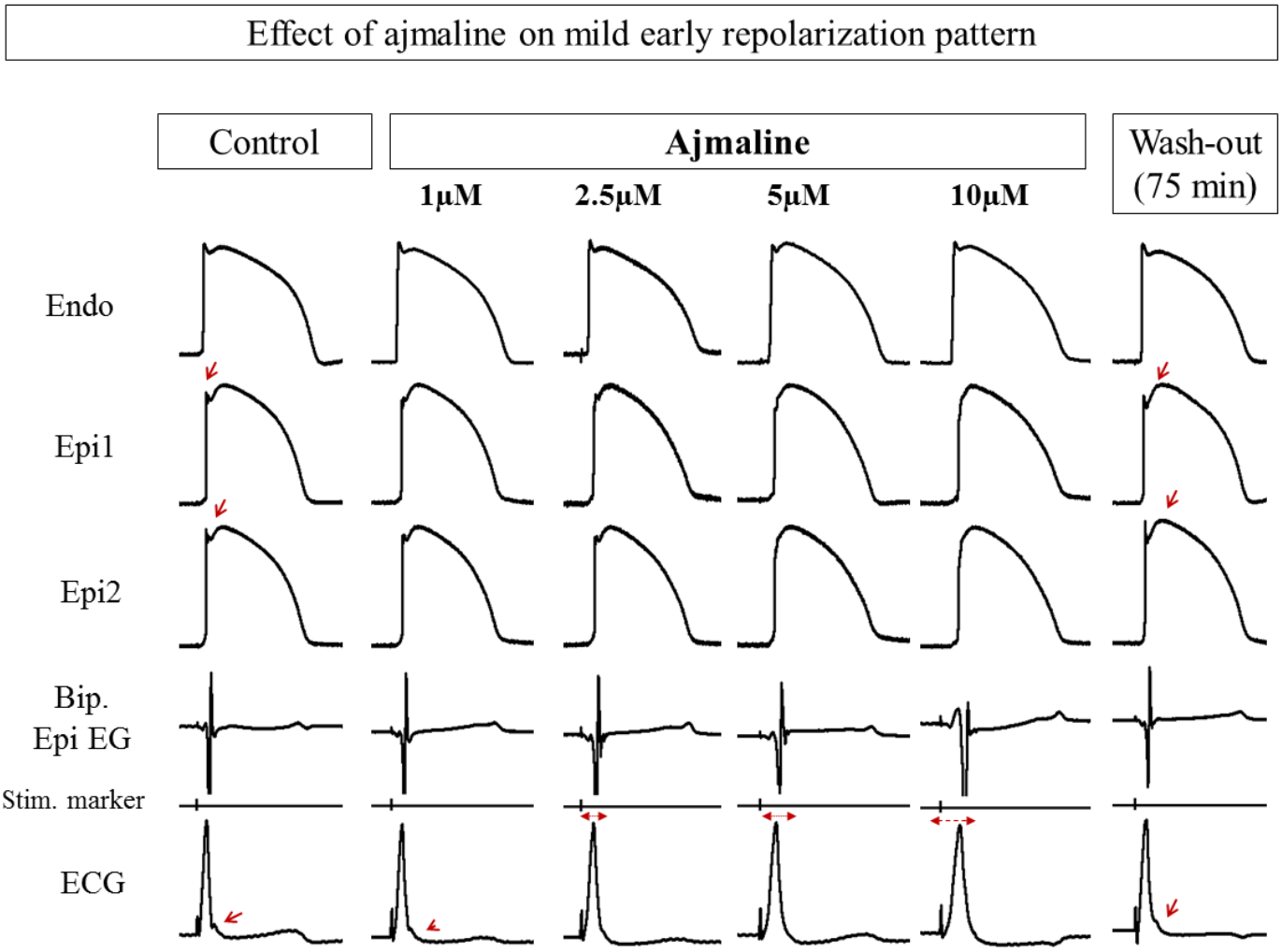


**Figure 15**: Ajmaline decreases early repolarization pattern displaying small J waves.
Canine left ventricular wedge preparation. Traces are denoted as in figure 14. Prolongation of QRS duration and diminished epicardial action potential notch led to disappearence of the J wave. The effects were reversible upon washout. These results explain the clinical observations of Bastiaenen et al. and Roten et al. [Bastiaenen 2013, Roten 2012], who reported improvement of early repolarization pattern in response to ajmaline. [from Patocskai 2016 JACC-EP]

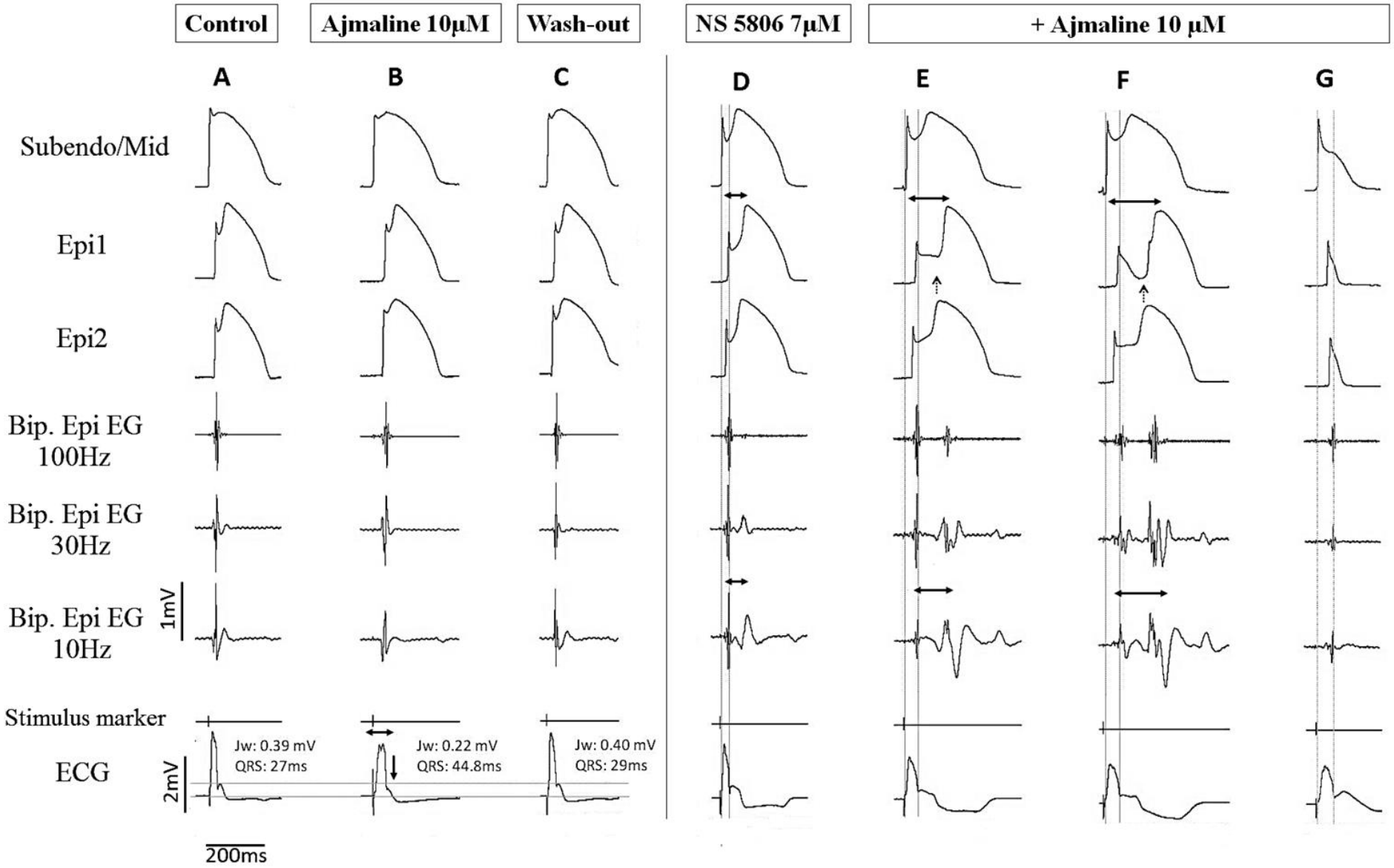
Control
Ajmaline 10µM
Wash-out
NS 5806 7µM
+ Ajmaline 10 µM
A
B
C
D
E
F
G
Subendo/Mid
Epi1
Epi2
Bip. Epi EG 100Hz
Bip. Epi EG 30Hz
Bip. Epi EG 10Hz
1mV
Stimulus marker
ECG
2mV
Jw: 0.39 mV
QRS: 27ms
Jw: 0.22 mV
QRS: 44.8ms
Jw: 0.40 mV
QRS: 29ms
200ms

**Figure 16:** The basal level of $I_{to}$-mediated action potential (AP) notch determines the dual effects of ajmaline to mask or accentuate the J wave. Each column represents simultaneous recordings of arterially perfused right ventricular wedge preparation. Subendo/Mid: APs from the subendocardium/midmyocardium. Bipolar surface-electrograms (Bip. Epi EG) were recorded from the epicardium using 3 different low cut filter settings (10Hz, 30Hz and 100Hz) and 250Hz "high cut" filter. Other traces are as described in Figure 14. When AP notch was small (**A**), 10 μM ajmaline produced a decrease in J wave -and AP notch area (**B**). The effect was reversible upon wash-out (**C**). However when the AP notch was amplified using the $I_{to}$ agonist NS5806 (**D**), the same concentration of ajmaline caused a marked accentuation of the J wave appearing as an ST segment elevation(**E, F, G**). Fragmented electrogram activity developed progressively as the repolarization defects became more pronounced and heterogeneous (**D, E, F**). Pronounced AP notch (without re-entry) produced delayed potentials in a lower frequency range (**D**), whereas phase 2 reentry depicted as "high-frequency" spike (**E, F**). After 15 min of ajmaline, loss of the action potential dome occurred throughout the preparation which led to disappearance of the late potentials (**G**). [from Patocskai 2016 JACC-EP]

### III.2. Effects of R- and S-mexiletine alone and in combination with sotalol

The effects of R-(-) and S-(+) mexiletine (20 μM) alone or in co-administration with sotalol (20 μM) on the AP parameters of dog papillary muscles paced at a stimulation cycle length of 1000 ms are summarized in Table 3, and illustrated in Figures 17 and 18 with representative traces.
None of these treatments changed the maximum diastolic potential (MDP), AP amplitude (APA), maximum rising velocity of the AP upstroke (Vmax) or conduction time (CT).

In single application, sotalol significantly lenghtened AP duration measured at 90% of repolarization ($APD_{90}$), whereas both enantiomers of mexiletine reduced Vmax and mildly shortened $APD_{90}$. When co-administered with sotalol, both R-(-) and S-(+) mexiletine were capable of significantly moderating sotalol-induced AP-prolongation in a similar extent ($p=0.026$ for $\Delta APD_{90(\underline{\textbf{R-mexiletine}} + \text{sotalol})}$ vs. $\Delta APD_{90(\text{Sotalol})}$, $p=0.007$ for $\Delta APD_{90(\underline{\textbf{S-mexiletine}} + \text{sotalol})}$ vs. $\Delta APD_{90(\text{Sotalol})}$ and $p=0.2633$ for $\Delta APD_{90(\textbf{R}\text{-mexiletine} + \text{sotalol})}$ vs. $\Delta APD_{90(\textbf{S}\text{-mexiletine} + \text{sotalol})}$. Significant differences between the effects of mexiletine's dextro- and levo-rotatory isomers on the studied electrophysiological parameters could not be observed.

| PARAMETERS | MDP (mV) | APA (mV) | $APD_{50}$ (ms) | $APD_{90}$ (ms) | $V_{max}$ (V/s) | CT (ms) |
|---|---|---|---|---|---|---|
| Control<br>Sotalol 20 µM | -80.5 ± 2.8<br>-79.7 ± 4.8<br>(6) | 100.1 ± 1.4<br>100.8 ± 3.0<br>(6) | 185.1 ± 13.0<br>219.1 ± 18.1<br>(6) | 225.5 ± 12.9<br>273.0 ± 16.8*<br>(6) | 174.6 ± 28.6<br>166.0 ± 32.0<br>(6) | 6.1 ± 0.8<br>5.3 ± 0.8<br>(6) |
| Control<br>R – Mexiletine 20 µM | -83.0 ± 2.0<br>-82.7 ± 1.8<br>(9) | 116.2 ± 2.5<br>114.0 ± 3.0<br>(9) | 179.8 ± 8.4<br>169.7 ± 8.0<br>(9) | 216.3 ± 6.3<br>204.7 ± 6.7<br>(9) | 187.2 ± 19.7<br>161.8 ± 15.2<br>(9) | 4.8 ± 0.5<br>5.3 ± 0.5<br>(9) |
| Control<br>S – Mexiletine 20 µM | -85.2 ± 3.1<br>-85.7 ± 2.4<br>(7) | 116.5 ± 3.9<br>114.2 ± 4.4<br>(7) | 172.9 ± 4.9<br>172.0 ± 7.1<br>(7) | 220.0 ± 7.2<br>214.1 ± 6.0<br>(7) | 200.0 ± 15.4<br>186.3 ± 17.2<br>(7) | 6.5 ± 1.0<br>7.1 ± 1.1<br>(7) |
| Control<br>Sotalol 20µM +<br>R – Mexiletine 20 µM | -84.7 ± 1.6<br>-83.7 ± 1.3<br>(6) | 115. 7 ± 3.1<br>113. 5 ± 3.1<br>(6) | 176.3 ± 5.0<br>198.5 ± 4.7*<br>(6) | 218.5 ± 3.6<br>243.2 ± 5.7*<br>(6) | 185.5 ± 25.7<br>158.2 ± 30.4<br>(6) | 4.6 ± 0.7<br>4.9 ± 0.9<br>(6) |
| Control<br>Sotalol 20µM +<br>S – Mexiletine 20 µM | -87.3 ± 1.6<br>-86.6 ± 1.6<br>(7) | 117.0 ± 3.5<br>117.7 ± 3.7<br>(7) | 176.4 ± 10.4<br>190.5 ± 15.7<br>(7) | 217.2 ± 13.0<br>234.2 ± 20.0<br>(7) | 189.4 ± 28.5<br>189.4 ± 25.5<br>(7) | 5.2 ± 0.8<br>5.4 ± 0.7<br>(7) |

***Table 3*:** The electrophysiological effects of sotalol, R-mexiletine, S-mexiletine and their combination in canine papillary muscle preparations at basic cycle length of 1000 ms. Results are mean ± S.E.M. *p<0.05 vs Control. MDP, maximum diastolic potential; APA, action potential amplitude; $APD_{50}$, action potential duration at 50% of repolarization; $APD_{90}$, action potential duration at 90% of repolarization; $V_{max}$, maximum rising velocity of the action potential upstroke; ERP, effective refractory period; CT, conduction time; (n), number of observations (i.e., number of preparations obtained from different animals).

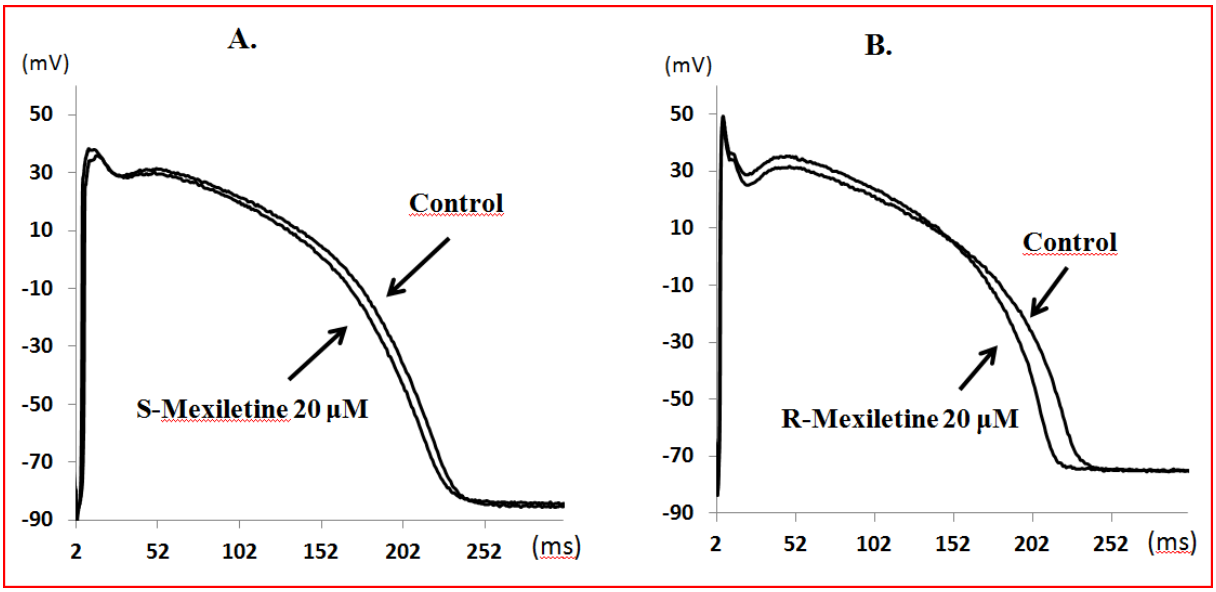


***Figure 17:*** Effects of the two enantiomers of mexiletine on action potential duration (APD). Representative traces recorded from superfused canine papillary muscle. Both R- and S-mexiletine caused a moderate shortening in APD.

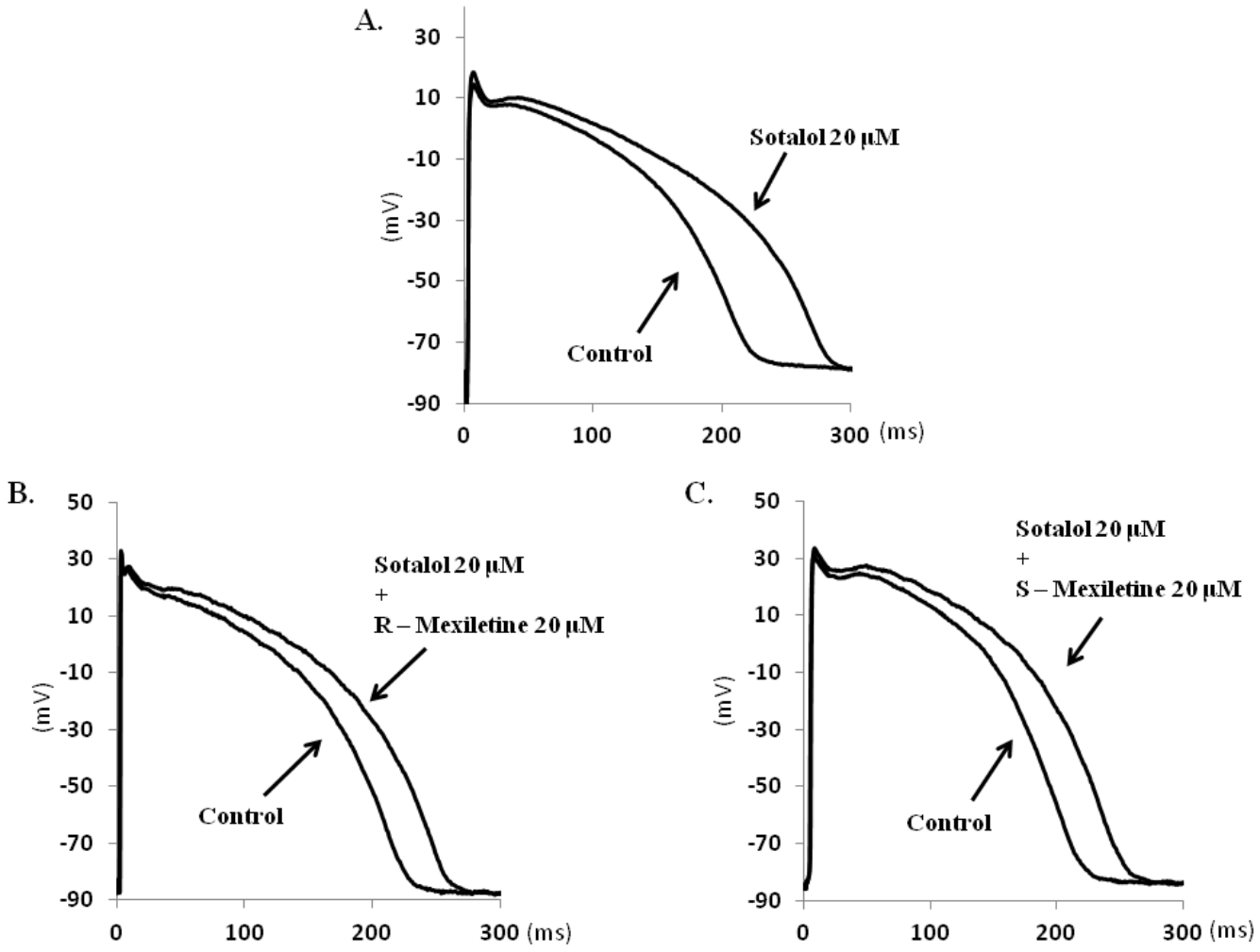


***Figure 18:*** Representative traces depicting the effect of sotalol applied alone (A) or combined with R-mexiletine (B) and S-mexiletine (C) on the morphology of canine papillary muscle action potential. Both enantiomers of mexiletine were able to moderate the prolonging effect of sotalol.

# IV. DISCUSSION

## IV.1 J wave syndromes

### *IV.1.1. Mechanisms underlying the action of cilostazol, mirinone and isoproterenol*

Our data indicates that both PDE3-inhibitors, cilostazol and milrinone, exert significant $I_{to}$-blocking action, pointing to this as an important mechanism for their ameliorative effect in ERS, in addition to their previously described virtue of augmenting $I_{Ca}$ [Atarashi 1998, Endoh 1986, Matsui

1999, Cone 1999]. We measured a 44.4% and 40.4 % reduction of $I_{to}$ at +40 mV in response to 10 μM of cilostazol and 2.5 μM of milrinone, respectively, in LV epicardial cardiomyocytes. The much greater potency of milrinone is consistent with the results of previous studies reporting that the same concentration of milrinone produces a greater increase in cytosolic cyclic adenosine monophosphate than does cilostazol [Cone 1999, Shakur 2002] possibly because milrinone blocks both PDE-3 and PDE-4 [Shakur 2002]. $I_{to}$ has previously been reported to be regulated by the cAMP/ phosphokinase-A pathway, suggesting that inhibition of $I_{to}$ may also apply to isoproterenol (and other sympathomimetics) in addition to its boosting effect on $I_{Ca}$ via direct stimulation of the beta adrenergic receptors. Although there is a relative consensus in that α1-adrenoceptor stimulation reduces $I_{to}$ current via $G_{\alpha s}$-mediated pathway [Apkon 1988, Ravens 1989, Martinez 2000, Gallego 2005], the net effect of acute β-adrenergic or general sympatethic stimulation under physiologic conditions is yet to be clarified [van der Heyden 2006]. Future experiments should be directed to test this hypothesis in human ventricular cardiomyocytes. It is noteworthy that cilostazol, milrinone and isoproterenol all produce positive inotropic and chronotropic effects. The elevation in heart rate would also be expected to indirectly decrease $I_{to}$ because the current is relatively slow to recover form inactivation. However, it also should be noted that all of these agents have the potential to enhance not only automaticity, but triggered activity as well, and thus may promote extrasystolic activity that may have unfavorable outcomes in certain cases [Kondo 2015].

Lately published studies from our group have provided evidence in support of a preferential accentuation of the AP notch in LV epicardium as the cellular basis for electrographic and arrhythmic manifestations of ERS [Koncz 2013]. Isolated accentuation of the epicardial but not endocardial AP notch leads to the development of transmural gradients across the LV wall and thereby the appearance of prominent J point elevation, distinct J waves, or slurring of the descending limb of the QRS complex.

In the present study, we pharmacologically modeled the genetic defects and attendant ionic changes with the use of verapamil to block $I_{Ca}$ and NS5806 to augment $I_{to}$. NS5806-induced augmentation of $I_{to}$ sensitized our preparations to the effects of verapamil consistent with the association of a higher density of this current in the inferior wall with a higher arrhythmic risk. Addition of verapamil further accentuates the AP notch, leading to the development of a more prominent J point and ST segment elevation. Increased concentration of these agents can then elicit all-or-none repolarization, leading to loss of the AP dome at some epicardial sites but not others (Figure 6), resulting in an epicardial dispersion of repolarization (EDR) (Figure 12; Table 2). Propagation of the AP dome from sites at which it was maintained to sites at which it was lost created a local re-excitation via a phase 2 reentry mechanism within the left ventricular epicardium.

Loss of the dome in the epicardium also creates a transmural dispersion of repolarization (TDR) giving rise to a vulnerable window across the ventricular wall which, when captured by a closely coupled extrasystole generated in the epicardium, induces VT/VF (Figures 9-11).

*IV.1.2. Mechanisms underlying the effect of ajmaline to unmask or blunt J wave*

The term J wave syndromes includes ERS and Brugada syndrome, because their electrocardiographic and arrhythmic manifestations are associated with accentuation of J waves. By testing the effects of ajmaline on ERS and Bugada syndrome models, our results point out again the crucial role of epicardial action potential notch in the pathophysiology of J wave syndromes. Depending on the size of the notch, ajmaline is capable of both diminishing and accentuating the pattern by its virtue to block both depolarizing currents like $I_{Na}$ and $I_{Ca}$ and repolarizing currents like $I_{to}$ and $I_{K\text{-}ATP}$ [Bebarova 2005]. In preparations exhibiting a relatively small action potential notch, ajmaline mildly diminished ERP (Figure 15) and failed to produce any sign of BrS (Figures 14B and 16B). These observations explain why ajmaline produces ST-elevation exclusively in the right precordial ECG leads of BrS patients (Figures 14A, 16E-G), but fails to provoke a Brugada pattern in other ECG-leads or in healthy subject, or in individuals with early repolarization pattern (Figure 15).

When the action potential notch was great enough, in addition to ajmaline's accentuating impact on Brugada syndrome ECG pattern, the drug prolonged the delay of late potentials in the epicardial bipolar electrogram recordings, as these post-QRS potentials were the depictions of the delayed 2$^{nd}$ upstrokes of the epicardial APs and phase 2 reentries. The splitting and fragmentation of the epicardial bipolar EG and appearance of late potentials following the addition of ajmaline is very similar to those recorded by Sacher et al. in the epicardium of the RVOT of a BrS patient [Sacher 2014]. Although their report interpreted this phenomenon as a proof of depolarization abnormality, in our experiments, ajmaline exerted these effects via accentuation of the AP notch and induction of P2R, and not via a conduction slowing (Figures 14A and and 16E-F). In support of this association, abnormal EG activity disappeared when the second upstroke of the AP and P2R has been lost homogeneously throughout the entire epicardium and subepicardium, despite further slowing of conduction (Figure 16-G). Our conclusion that late potentials were the consequence of repolarization defects was further verified by their behavior in response to cilostazol, milrinone and isoprotenol: all three agents concordantly suppressed the fragmentation, delay and amplitude of post-QRS potentials, secondary to their virtue of reducing of AP notch and terminating P2Rs.

Although repolarization models can recapitulate and explain every aspect of the syndrome, we have to emphasize that our studies are not aimed at proving the exclusivity of repolarization

hypothesis. There is no doubt that depolarization abnormalities can contribute to development of J waves and related arrhythmogenesis [Meijborg 2016, Hoogendijk 2013], and several factors can modulate the transmural heterogeneity and the degree of both repolarization and depolarization abnormalities, including electrotonic coupling, "source-sink" relationship, transmural differences in tissue resistivity and transmural and regional distribution of other ion channels and gap junctions [Yan 1998, LeGrice 1995, Liu 1995, Nguyen 2012, Xie 2010, Poelzing 2004, Yamada 2004, Gaborit 2007, Szabo 2005, Szentandrassy 2005, Rosati 2006, Soltysinska 2009, McKinnon 2016]. From one point of view, accentuated AP notch and phase 2 reentry, in turn, can be interpreted as a disruption between the two main *depolarizing* "pulses" of an AP, produced by a robust *repolarization* "pulse". In this aspect, regardless of the indirect or direct cause, it would be thoughtlessness to exclude the potential role of either repolarization or depolarization abnormality in the pathophysiology of J wave syndromes.

*IV.1.4. Limitations of the study*

We designed our pharmacologic models to mimic the genetic defects associated with ERS (or Brugada syndrome) and to test the effects of agents with therapeutic and unmasking potentials. To assay the effects of these compounds on every single known mutation associated with J wave syndromes is clearly beyond the scope of our (or any) study. Our pharmacological models may not perfectly mimic the phenotypic manifestation of every mutation, but they do serve to recapitulate the net result of the ion-current imbalance created and thus provide a reasonable platform to test the effects of PDE inhibitors, beta adrenergic agents or sodium channel blockers.

It would certainly be preferable to study the effect of these agents in transgenic animal models too, but none at present are capable of recapitulating the arrhythmic and electrographic manifestations of J wave syndromes. In a recent study, Park et al attempted to mimic Brugada syndrome phenotype in Yucatan minipigs by heterozygous expression of a nonsense mutation in SCN5A (E558X) identified in a child with Brugada syndrome [Park 2015]. Myocytes isolated from the $SCN5A^{E558X/+}$ pigs showed a loss of function of $I_{Na}$. Various conduction abnormalities were observed but not a BrS phenotype, not even after flecainide-test, because pigs lack the $I_{to}$ current and AP notch in ventricular cardiomyocytes. These observations point to the crucial importance of $I_{to}$ in the development of J wave syndrome phenotype. Transgenic mice are not helpful because the fundamental differences in their repolarization characteristics.

It might also be contended that arterially perfused wedge preparations do not cover the complete anatomical and electrical structure of the heart and thus may not fully recapitulate the

disease phenotype, i.e., artificial stimulation and the lack of the His-Purkinje system may alter the normal activation pattern.

However, all these possible objections may be counter-argued by the fact that the arterially perfused ventricular wedge preparation is currently the only model capable of recapitulating all features of ERS and BrS (e.g., response to pharmacologic agents, response to ablation, response to changes in heart rate and electrographic and arrhythmic manifestations). This model has pioneered in permitting researchers to elucidate the cellular mechanisms and thus to recommend novel therapeutic approaches in several cardiac diseases. Studies conducted on these models were the first to recommend the use of quinidine and isoproterenol for the treatment of the J wave syndromes [Yan 1999], which are widely used in the clinical practice today to deal with J wave syndrome-associated electrical storms or as an adjunct to ICD therapy. These models have also identified ECG markers such as Tpeak-Tend and QT/RR relationships that have proved useful in risk stratification of patients with LQTS, BrS and SQTS [Extramiana 2004, Antzelevitch 2006, Antzelevitch 2007, Patel 2008,].

As with any study involving experimental animal models, extrapolation of the data to the clinic must be approached with great caution.

### IV.2. Enantiomers of mexiletine and their co-administration with sotalol

Previously [Gurabi 2017] our research group analysed the effects of R-(-) and S-(+) enantiomers of mexiletine on AP parameters in rabbit right ventricular papillary muscle preparations. We have found that R-(-) optical isomer displays a tendency to a more potent inhibitory effect on Vmax when compared to the S-(+) stereoisomer.

In our present work, our primary aim was to compare the ability of the two enantiomers to abbreviate APD, especially when APD is abnormally prolonged secondary to an „acquired" condition, i.e. $I_{Kr}$-block by sotalol. A possibly more pronounced AP shortening effect of one of the enantiomers would have a remarkable clinical impact. A recent study by Badri et al. reported that mexiletine is a promising treatment approach to terminate refractory TdP tachyarrhthmia in several acquired forms of LQTS [Badri 2015]. A mexiletine enantiomer with higher abbreviating-potency would supposedly offer a more effective therapeutic option for these individuals.

In our recent study, performed on isolated canine papillary muscle preparation, significant differences in the effects of mexiletine's levo- and dextrorotatory isomers could not be observed, suggesting that the separate application of neither enantiomer offers a therapeutic advantage

compared to the use of the racemic form. However, it has to be emphasized that we cannot exclude the possibility that in human heart or in cardiomyocytes of other ventricular regions, layers or functions, the two optical isomers would display meaningfully divergent electrophysiological effects. It is also noteworthy that we did not implement direct tests on TdP- or other arrhythmia models; therefore or conslusions are extrapolative. Further researches in this field are most welcome.

## V. ACKNOWLEDGEMENT

I would like to seize the opportunity to express my gratitude to Dr. István Koncz for introducing me in cardiac research and for his superlative professional mentorship throughout my scientific career. The work investigating the "Effects of R- and S-mexiletine alone and in combination with sotalol" was supported by the ÚNKP-ÚNKP-16-4 New National Excellence Program of the Ministry of Human Capacities, Hungary. My sincere thanks go to Prof. Dr. András Varró for his continuous support as well as to Dr. Zsolt Gurabi, Dr. José Di Diego and Dr. Serge Sicouri for their kind technical assistance.

I am especially grateful to Prof. Dr. Charles Antzelevitch for his exceptional scientific guidance and for giving me and my supervisor, Dr. István Koncz, the opportunity to work in a superbly competent milieu in the Masonic Medical Research Laboratory (Utica, NY, USA).

VI. REFERENCES

Aizawa Y, Sato A, Watanabe H, Chinushi M, Furushima H, Horie M, Kaneko Y, Imaizumi T, Okubo K, Watanabe I, Shinozaki T, Aizawa Y, Fukuda K, Joo K, Haissaguerre M.
Dynamicity of the J-wave in idiopathic ventricular fibrillation with a special reference to pause-dependent augmentation of the J-wave. J Am Coll Cardiol. 2012 May 29;59(22):1948-53.

Aizawa Y, Chinushi M, Hasegawa K, Naiki N, Horie M, Kaneko Y, Kurabayashi M, Ito S, Imaizumi T, Aizawa Y, Takatsuki S, Joo K, Sato M, Ebe K, Hosaka Y, Haissaguerre M and Fukuda K. Electrical storm in idiopathic ventricular fibrillation is associated with early repolarization. J Am Coll Cardiol. 2013;62:1015-1019.

Aizawa Y, Sato M, Kitazawa H, Aizawa Y, Takatsuki S, Oda E, Okabe M, Fukuda K. Tachycardia-dependent augmentation of "notched J waves" in a general patient population without ventricular fibrillation or cardiac arrest: Not a repolarization but a depolarization abnormality? Heart Rhythm. 2015; 12:376–83.

Alders M, Koopmann TT, Christiaans I, et al. Haplotype-sharing analysis implicates chromosome 7q36 harboring DPP6 in familial idiopathic ventricular fibrillation.Am J Hum Genet 2009; 84: 468–476.

Antzelevitch C, Oliva A. Amplification of spatial dispersion of repolarization underlies sudden cardiac death associated with catecholaminergic polymorphic VT, long QT, short QT and Brugada syndromes. J Intern Med 2006;259:48-58.

Antzelevitch C, Pollevick GD, Cordeiro JM, et al. Loss-of-function mutations in the cardiac calcium channel underlie a new clinical entity characterized by ST-segment elevation, short QT intervals, and sudden cardiac death. Circulation 2007; 115: 442–449.

Antzelevitch C, Sicouri S, Di Diego JM et al. Does $T_{peak}$-$T_{end}$ provide an index of transmural dispersion of repolarization? Heart Rhythm 2007;4:1114-1116.
Antzelevitch C, Patocskai B. Brugada Syndrome: Clinical, Genetic, Molecular, Cellular, and Ionic Aspects.Curr Probl Cardiol. 2016 Jan;41(1):7-57.

Antzelevitch C, Patocskai B. Ionic and Cellular Mechanisms Underlying the J wave Syndromes. Book chapter in: J wave syndromes. Springer International Publishing Switzerland 2016. ISBN 978-3-319-31576-8 ISBN 978-3-319-31578-2 (eBook) DOI 10.1007/978-3-319-31578-2 Library of Congress Control Number: 2016942096

Apkon M, Nerbonne JM. α1-Adrenergic agonists selectively suppress voltage-dependent K+ currents in rat ventricular myocytes. Proc Natl Acad Sci USA, 1988, 85(22):8756-60.

Arita M, Goto M, Nagamoto Y, and Saikawa T. Electrophysiological actions of mexiletine (Kö1173) on canine Purkinje fibres and ventricular muscle. Br. J. Pharmacol. 1979.67(1): 143-52

Atarashi H, Endoh Y, Saitoh H, Kishida H, Hayakawa H. Chronotropic effects of cilostazol, a new antithrombotic agent, in patients with bradyarrhythmias. J Cardiovasc Pharmacol 1998; 31: 534–539.

Badri M, Patel A, Patel C, Liu G, Goldstein M, Robinson VM, Xue X, Yang L, Peter R. Kowey PR, Yan GX. Mexiletine prevents recurrent Torsades de Pointes in acquired long QT syndrome refractory to conventional measures. JACC Clin. Electrophysiol. 2015. 1(4): 315-322.

Barajas-Martinez H, Hu D, Ferrer T, et al. Molecular genetic and functional association of Bugada and early repolarization syndromes with S422L missense mutation in KCNJ8. Heart Rhythm 4/1/2012 2012; 9:548-555

Barajas-Martinez H, Hu D, Pfeiffer R, Burashnikov E, Powers A, Knilans TK, Antzelevitch C. A genetic variant in DPP10 linked to inherited J-wave syndrome associated with sudden cardiac death by augmentation of Kv4.3channel current. Heart Rhythm 2012; 9:1919–1920

Bardy GH, Smith WM, Hood MA, Crozier IG, Melton IC, Jordaens L, Theuns D, Park RE, Wright DJ, Connelly DT, Fynn SP, Murgatroyd FD, Sperzel J, Neuzner J, Spitzer SG, Ardashev AV, Oduro A, Boersma L, Maass AH, Van Gelder IC, Wilde AA, van Dessel PF, Knops RE, Barr CS, Lupo P, Cappato R, Grace AA. An entirely subcutaneous implantable cardioverter-defibrillator. N Engl J Med 2010; 363:36-44

Bastiaenen R, Hedley PL, Christiansen M, Behr ER. Therapeutic hypothermia and ventricular fibrillation storm in early repolarization syndrome. Heart Rhythm 2010; 7:832-834.

Bastiaenen R, Raju H, Sharma S, Papadakis M, Chandra N, Muggenthaler M, Govindan M, Batchvarov VN, Behr ER. Characterization of early repolarization during ajmaline provocation and exercise tolerance testing. Heart Rhythm 2013; 10:247-254.

Bébarová M, Matejovič P, Pásek M, Šimurdová M and Šimurda J. Effect of Ajmaline on Action Potential and Ionic Currents in Rat Ventricular Myocytes. Gen. Physiol. Biophys. 2005, 24, 311—325

Bien H, Yin L, Entcheva E. Calcium instabilities in mammalian cardiomyocyte networks. Biophysical journal. 2006; 90:2628-2640

Brosnan MJ, Kumar S, LaGerche A, Brown A, Stewart S, Kalman JM, Prior DL. Early repolarization patterns associated with increased arrhythmic risk are common in young non-Caucasian Australian males and not influenced by athletic status. Heart Rhythm 2015;12:1576–1583.

Burashnikov E, Pfeiffer R, Barajas-Martinez H, et al. Mutations in the cardiac L-type calcium channel associated J wave sydnrome and sudden cardiac death. Heart Rhythm 12/2010 2010;7:1872-1882.

Calloe K, Cordeiro JM, Di Diego JM, Hansen RS, Grunnet M, Olesen SP, Antzelevitch C. A transient outward potassium current activator recapitulates the electrocardiographic manifestations of Brugada syndrome. Cardiovasc Res. 2009 Mar 1;81(4):686-94.

Campbell TJ. Resting and rate-dependent depression of maximum rate of depolarisation (Vmax) in guinea pig ventricular action potentials by mexiletine, disopyramide, and encainide. J. Cardiovasc. Pharmacol. 1983. 5(2): 291-6.

Chézalviel-Guilbert F, Davy JM, Poirier JM, Weissenburger J. Mexiletine antagonizes effects of sotalol on QT interval duration and its proarrhythmic effects in a canine model of torsade de pointes. J Am Coll Cardiol. 1995. 26(3):787-92. PMID: 7642874

Chialvo DR, Gilmour RF Jr., Jalife J. Low dimensional chaos in cardiac tissue. Nature. 1990; 343:653-657

Cone J, Wang S, Tandon N, Fong M, Sun B, Sakurai K, Yoshitake M, Kambayashi J, Liu Y. Comparison of the effects of cilostazol and milrinone on intracellular cAMP levels and cellular function in platelets and cardiac cells. J Cardiovasc Pharmacol 1999; 34:497–504.

De Luca A, Natuzzi F, Lentini G, Franchini C, Tortorella V, and Conte Camerino D. Stereoselective effects of mexiletine enantiomers on sodium currents and excitability characteristics of adult skeletal muscle fibers. Naunyn-Schmiedeberg's Arch. Pharmacol. 1995. 352(6): 653-61

De Maria E, Bonetti L, Patrizi G, et al. Implantation of a completely subcutaneous ICD system: case report of a patient with Brugada syndrome and state of the art. J Interv Card Electrophysiol 2012; 34:105-13

Demidova MM, Martin-Yebra A, van der Pals J, Koul S, Erlinge D, Laguna P, Martinez JP, Platonov PG. Transient and rapid QRS-widening associated with a J-wave pattern predicts impending ventricular fibrillation in experimental myocardial infarction. Heart Rhythm 2014; 11:1195–1201.

Derval N et al. Prevalence and characteristics of early repolarization in the CASPER registry: cardiac arrest survivors with preserved ejection fraction registry. J Am Coll Cardiol 2011; 58:722–728.

Di Diego JM, Sun ZQ, Antzelevitch C. I(to) and action potential notch are smaller in left vs. right canine ventricular epicardium. The American journal of physiology. 1996; 271:H548-561

Endoh M,Yanagisawa T, Taira N, Blinks JR. Effects of new inotropic agents on cyclic nucleotide metabolism and calcium transients in canine ventricular muscle. Circulation 1986; 73:III117–III133.

Ermakov S, Hoffmayer KS, Gerstenfeld EP, Scheinman MM. Combination drug therapy for patients with intractable ventricular tachycardia associated with right ventricular cardiomyopathy. Pacing Clin Electrophysiol. 2014 Jan; 37(1):90-4.

Extramiana F, Antzelevitch C. Amplified transmural dispersion of repolarization as the basis for arrhythmogenesis in a canine ventricular-wedge model of short QT syndrome. Circulation 2004; 110:3661-3666.

Federman NJ, Mechulan A, Klein GJ, Krahn AD. Ventricular fibrillation induced by spontaneous hypothermia in a patient with early repolarization syndrome. J Cardiovasc Electrophysiol 2013; 24:586-588.

Gaborit N, Le Bouter S, Szűts V, Varró A, Escande D, Nattel S, Demolombe S.
Regional and tissue specific transcript signatures of ion channel genes in the non-diseased human heart. J Physiol. 2007 Jul 15; 582(Pt 2):675-93

Gallego M, Setien R, Puebla L, Boyano-Adanez MC, Arilla E, Casis O. Alpha1-Adrenoceptors stimulate a Galphas protein and reduce the transient outward $K^+$ current via a cAMP/PKA-mediated pathway in the rat heart. Am J Physiol Cell Physiol 3/2005 2005; 288:C577-C585.

Gao Y, Xue X, Hu D, Liu W, Yuan Y, Sun H, et al. Inhibition of late sodium current by mexiletine: a novel pharmotherapeutical approach in Timothy syndrome. Circ. Arrhythm. Electrophysiol. 2013; 6(3): 614-22.

Giudicessi JR,Ye D, Kritzberger CJ, Nesterenko VV, Tester DJ, Antzelevitch C, Ackerman MJ. Novel mutations in the KCND3-encoded Kv4.3 $K^+$ channel associated with autopsy-negative sudden unexplained death. Hum Mutat 2012; 33:989–997.

Ghosh S, Cooper DH, Vijayakumar R, Zhang J, Pollak S, Haissaguerre M, Rudy Y. Early repolarization associated with sudden death: insights from noninvasive electrocardiographic imaging. Heart Rhythm. 2010; 7:534–7.

Griksaitis MJ, Rosengarten JA, Gnanapragasam JP, et al. Implantable cardioverter defibrillator therapy in paediatric practice: a single-centre UK experience with focus on subcutaneous defibrillation. Europace 2013;15:523-30

Gussak I, Antzelevitch C. Early repolarization syndrome: clinical characteristics
and possible cellular and ionic mechanisms. J Electrocardiol 2000; 33:299 –309.

Gurabi Z, Patocskai B, Györe B, Virág L, Mátyus P, Papp JG, Varró A, Koncz I.
Different electrophysiological effects of the levo- and dextrorotatory isomers of mexiletine in isolated rabbit cardiac muscle. Canadian Journal of Physiology and Pharmacology. 2017 Feb. doi: 10.1139/cjpp-2016-0599. [Epub ahead of print]

Haissaguerre M et al. Sudden cardiac arrest associated with early repolarization. N Engl J Med 2008; 358:2016–2023.

Haissaguerre et al. Characteristics of recurrent ventricular fibrillation associated with inferolateral early repolarization role of drug therapy. J Am Coll Cardiol 2009; 53:612–619.

Haissaguerre M, Chatel S, Sacher F, et al. Ventricular fibrillation with prominent early repolarization associated with a rare variant of KCNJ8/$K_{ATP}$ channel. J Cardiovasc Electrophysiol 2009; 20:93-98.

Hamill OP, Marty A, Neher E, Sakmann B, Sigworth FJ. Improved patch–clamp techniques for high-resolution current recording from cells and cell-free membrane patches. Pflugers Arch 1981; 391:85–100.

Haruta D, Matsuo K, Tsuneto A, Ichimaru S, Hida A, Sera N, Imaizumi M, Nakashima E, Maemura K, Akahoshi M. Incidence and prognostic value of early repolarization pattern in the 12–lead electrocardiogram. Circulation 2011; 123: 2931–2937.

Hayashi M, ShimizuW, Albert CM. The spectrum of epidemiology underlying sudden

cardiac death. Circ Res 2015;116:1887–1906.

Hering S, Bodewei R, and Wollenberger A. Sodium current in freshly isolated and in cultured single rat myocardial cells: frequency and voltage-dependent block by mexiletine. J. Mol. Cell. Cardiol.1983; 15(7): 431-44

Hohnloser S, Weirich J, and Antoni H. Effects of mexiletine on steady-state characteristics and recovery kinetics of V max and conduction velocity in guinea pig myocardium. J. Cardiovasc. Pharmacol. 1982; 4(2): 232-9.

Hoogendijk MG, Potse M, and Coronel R. Critical appraisal of the mechanism underlying J waves. J. Electrocardiol. 2013; 46, 390–394.

Hu D, Barajas-Martinez H, Medeiros-Domingo A, etal. A novel rare variant in SCN1Bb linked to Brugada syndrome and SIDS by combined modulation of Na(v)1.5 and K(v)4.3 channel currents. Heart Rhythm 2012; 9:760–769.

Hu D, Barajas-Martinez H, Terzic A, et al. ABCC9 is a novel Brugada and early repolarization syndrome susceptibility gene. Int J Cardiol. 2014; 171:431-442.

Hu D, Barajas-Martinez H, Pfeiffer R, et al. Mutations in SCN10A are responsible for a large fraction of cases of Brugada syndrome. J Am Coll Cardiol. 2014; 64: 66-79.

Huikuri HV. Separation of Benign from Malignant J waves. Heart Rhythm. 2015; 12:384–5.

Iguchi K, Noda T, Kamakura S and Shimizu W. Beneficial effects of cilostazol in a patient with recurrent ventricular fibrillation associated with early repolarization syndrome.
Heart Rhythm. 2013; 10:604-606.

Kalla H, Yan GX, Marinchak R. Ventricular fibrillation in a patient with prominent J (Osborn) waves and ST segment elevation in the inferior electrocardiographic leads: a Brugada syndrome variant? J Cardiovasc Electrophysiol 2000; 11:95–8.

Kambara H, Phillips J. Long-term evaluation of early repolarization syndrome (normal variant RS-T segment elevation). Am J Cardiol 1976; 38:157–161.

Kaneko Y, Horie M, Niwano S, Kusano K, Takatsuki S, Kurita T, Mitsuhashi T, Nakajima T, Irie T, Hasegawa K, Noda T, Kamakura S, Aizawa Y, Yasuoka R, Torigoe K, Suzuki H, Ohe T, Shimizu A, Fukuda K, Kurabayashi M, Aizawa Y. Electrical storm in patients with Brugada syndrome is associated with early repolarization. Circ Arrhythm Electrophysiol. 2014; 7:1122–8.

Karagueuzian HS, Stepanyan H, Mandel WJ. Bifurcation theory and cardiac arrhythmias. American journal of cardiovascular disease. 2013; 3:1-16

Katsuumi G, Shimizu W, Watanabe H, Noda T, Nogami A, Ohkubo K, Makiyama T, Takehara N, Kawamura Y, Hosaka Y, Sato M, Fukae S, Chinushi M, Oda H, Okabe M, Kimura A, Maemura K, Watanabe I, Kamakura S, Horie M, Aizawa Y, Makita N, MinaminoT. Efficacy of bepridil to prevent ventricular fibrillation in severe form of early repolarization syndrom e. Int J Cardiol. 2014 Mar 15;172(2):519-22.

Kawata H, Morita H, Yamada Y, Noda T, Satomi K, Aiba T, Isobe M, Nagase S, Nakamura K, Fukushima KK, Ito H, Kamakura S, and Shimizu W.
Prognostic significance of early repolarization in inferolateral leads in Brugada patients with documented ventricular fibrillation: a novel risk factor for Brugada syndrome with ventricular fibrillation. Heart Rhythm 2013; n10: 1161-1168.

Kim SH, Nam GB, Baek S. Circadian and seasonal variations of ventricular tachyarrhythmias in patients with early repolarization syndrome and Brugada syndrome: analysis of patients with implantable cardioverter defibrillator. J Cardiovasc Electrophysiol. 2012;23:757–763.

Klatsky AL, Oehm R, Cooper RA, Udaltsova N, Armstrong MA. The early repolarization normal variant electrocardiogram: correlates and consequences. Am J Med 2003;115:171.

Koncz I, Gurabi Z, Patocskai B, Panama BK, Szél T, Hu D, Barajas-Martínez H, Antzelevitch C. Mechanisms underlying the development of the electrocardiographic and arrhythmic manifestations of early repolarization syndrome.
Journal of Molecular and Cellular Cardiology, 2014 Mar; 68:20-8.

Kondo H, Shinohara T, Takahashi N. A case of short-coupled premature ventricular beat-induced ventricular fibrillation with early repolarization in the inferolateral leads.
J Arrhythm 2015; 31:60–63.

Kraus F. Ueber die Wirkung des Kalziums auf den Kreislauf.
Dtsch Med Wochenschr. 1920; 46:201-203.

LeGrice IJ, Smaill BH, Chai LZ, Edgar SG, Gavin JB, Hunter PJ. Laminar structure of the heart: ventricular myocyte arrangement and connective tissue architecture in the dog.
Am J Physiol 1995; 269:H571–82.

Lerma C, Krogh-Madsen T, Guevara M, Glass L. Stochastic aspects of cardiac arrhythmias.
J Stat Phys. 2007; 128: 347–374.

Letsas KP, Efremidis M, Pappas LK, et al. Early repolarization syndrome: is it always benign? Int J Cardiol 2007;114:390 –392.

Letsas KP, Sacher F, Probst V, Weber R, Knecht S, Kalusche D, Haissaguerre M and Arentz T. Prevalence of early repolarization pattern in inferolateral leads in patients with Brugada syndrome. Heart Rhythm. 2008; 5:1685-1689.

Litovsky SH, Antzelevitch C. Transient outward current prominent in canine ventricular epicardium but not endocardium. Circ Res 1988; 62:116 –126.

Liu DW, Antzelevitch C. Characteristics of the delayed rectifier current (IKr and IKs) in canine ventricular epicardial, midmyocardial, and endocardial myocytes. A weaker IKs contributes to the longer action potential of the M cell. Circ Res 1995; 76:351–65.

Logigian EL, Martens WB, Moxley RT, McDermott MP, Dilek N, Wiegner AW, et al. Mexiletine is an effective antimyotonia treatment in myotonic dystrophy type 1.
Neurology 2010; 74(18): 1441-8.

Lu YY, Chung FP, Chen YC, Tsai CF, Kao YH, Chao TF, Huang JH, Chen SA, Chen YJ.

Distinctive electrophysiological characteristics of right ventricular outflow tract cardiomyocytes. J Cell Mol Med. 2014 Aug; 18(8):1540-8. doi: 10.1111/jcmm.12329.

Macfarlane PW, Antzelevitch C, Haissaguerre M, Huikuri HV, Potse M, Rosso R, Sacher F, Tikkanen JT, Wellens H, Yan GX. The Early Repolarization Pattern: A Consensus Paper. J Am Coll Cardiol Jul 28 2015;66:470-477.

Maeda S, Takahashi Y, Nogami A, Yamauchi Y, Osaka Y, Shirai Y, Ihara K, Yokoyama Y, Suzuki M, Okishige K, Nishizaki M, Hirao K. Seasonal, weekly, and circadian distribution of ventricular fibrillation in patients with J-wave syndrome from the J-PREVENT registry. J Arrhythm. 2015 Oct;31(5):268-73.

Maoz A, Krogh-Madsen T, Christini DJ. Instability in action potential morphology underlies phase 2 reentry: A mathematical modeling study. Heart rhythm 2009; 6:813-822

Maoz A, Christini DJ, Krogh-Madsen T. Dependence of phase-2 reentry and repolarization dispersion on epicardial and transmural ionic heterogeneity: A simulation study. Europace : European pacing, arrhythmias, and cardiac electrophysiology : journal of the working groups on cardiac pacing, arrhythmias, and cardiac cellular electrophysiology of the European Society of Cardiology. 2014; 16:458-465

Martinez ML, Delgado C. Methoxamine inhibits transient outward potassium current through α1A-adrenoceptors in rat ventricular myocytes J Cardiovasc Pharmacol 2000; 35: 212-218.

Mason JW. A comparison of seven antiarrhythmic drugs in patients with ventricular tachyarrhythmias. Electrophysiologic Study versus Electrocardiographic Monitoring Investigators. N. Engl. J. Med. 1993. 329(7): 452-8.

Matsui K, Kiyosue T, Wang JC, Dohi K, Arita M. Effects of pimobendan on the L-type Ca2+ current and developed tension in guinea-pig ventricular myocytes and papillary muscle: comparison with IBMX, milrinone, and cilostazol. Cardiovasc Drugs Ther 1999; 13:105–113.

Maury P, Rollin A. Prevalence of early repolarisation/J wave patterns in the normal population. J Electrocardiol. 2013 Sep-Oct;46(5):411-6.

McKinnon D, Rosati B. Transmural gradients in ion channel and auxiliary subunit expression. Prog Biophys Mol Biol. 2016 Dec; 122(3):165-186

Medeiros-Domingo A, Tan BH, Crotti L, et al. Gain-of-function mutation S422L in the KCNJ8-encoded cardiac K(ATP) channel Kir6.1 as a pathogenic substrate for J-wave syndromes. Heart Rhythm 2010; 7:1466-1471.

Mehta MC, Jain AC. Early repolarization on scalar electrocardiogram. Am J Med Sci 1995; 309:305.

Meijborg VM, Potse M, Conrath CE, Belterman CN, De Bakker JM, Coronel R. Reduced Sodium Current in the Lateral Ventricular Wall Induces Inferolateral J-Waves. Front Physiol. 2016 Aug 26;7:365.

Mizumaki K, Nishida K, Iwamoto J. Vagal activity modulates spontaneous augmentation of J-wave elevation in patients with idiopathic ventricular fibrillation. Heart Rhythm. 2012; 9:249–255.

Nam GB, Kim YH, Antzelevitch C. Augmentatin of J waves and electrical storms in patients with early repolarization. N Engl J Med 2008; 358:2078–2079.

Napolitano C, Antzelevitch C. Phenotypical manifestations of mutations in the genes encoding subunits of the voltage dependent L-type calcium channel. Circ Res 2011; 108:607-618.

Nattel S and Carlsson L. Innovative approaches to anti-arrhythmic drug therapy
Nature Reviews Drug Discovery 2006 Dec; 5, 1034-1049.

Nguyen TP, Xie Y, Garfinkel A, Qu Z, Weiss JN. Arrhythmogenic consequences of myofibroblast-myocyte coupling. Cardiovasc Res 2012; 93:242–51.

Noseworthy PA, et al. The early repolarization pattern in the general population: clinical correlates and heritability. J Am Coll Cardiol 2011; 57:2284–2289.

O'Connor AB, and Dworkin RH. Treatment of neuropathic pain: an overview of recent guidelines. Am. J. Med. 2009; 122(10 Suppl): S22-32.

Osborn JJ. Experimental hypothermia: respiratory and blood pH changes in relation to cardiac function. Am J Physiol. 1953; 175:389-398.

Park HJ, and Moon DE. Pharmacologic management of chronic pain. Korean J. Pain 2010; 23(2): 99-108.

Park DS, Cerrone M, Morley G, et al. Genetically engineered SCN5A mutant pig hearts exhibit conduction defects and arrhythmias. J Clin Invest 2015; 125: 403–412.

Patel C, Antzelevitch C. Cellular basis for arrhythmogenesis in an experimental model of the SQT1 form of the short QT syndrome. Heart Rhythm 2008; 5:585-590.

Patel RB, Ng J, Reddy V, Chokshi M, Parikh K, Subacius H, Alsheikh-Ali AA, Nguyen T, Link MS, Goldberger JJ, Ilkhanoff L, Kadish AH. Early repolarization associated with ventricular arrhythmias in patients with chronic coronary artery disease. Circ Arrhythm Electrophysiol. 2010 Oct; 3(5):489-95.

Patel RB, Ilkhanoff L, Ng J, Chokshi M, Mouchli A, Chacko SJ, Subacius H, Bhojraj S, Goldberger JJ, Kadish AH. Clinical characteristics and prevalence of early repolarization associated with ventricular arrhythmias following acute ST-elevation myocardial infarction. Am J Cardiol. 2012 Sep 1; 110(5):615-20.

Patocskai B, Koncz I, Gurabi Z, Antzelevitch C. Cellular mechanisms underlying the effect of cilostazol, milrinone and isoproterenol to supress arrhythmogenesis in an experimental model of early repolarization syndrome.[Oral presentation] In: Program and abstracts of the 23rd Annual Meeting of the Upstate New York Cardiac Electrophysiology Society and Upper Canada Cardiac Electrophysilogy Society; October 11, 2013, Toronto, Canada

Patocskai B and Antzelevitch C. Novel therapeutic strategies for the management of ventricular arrhythmias associated with the Brugada syndrome.
Expert Opin Orphan Drugs. 2015; 3(6):633-651.

Patocskai B, Barajas-Martinez H, Hu D, Gurabi Z, Koncz I, Antzelevitch C.
Cellular and ionic mechanisms underlying the effects of cilostazol, milrinone, and isoproterenol to suppress arrhythmogenesis in an experimental model of early repolarization syndrome. Heart Rhythm. 2016 Jun; 13(6):1326-34.

Patocskai B, Yoon N, Antzelevitch C. Mechanisms Underlying Epicardial Radiofrequency Ablation to Suppress Arrhythmogenesis in Experimental Models of Brugada Syndrome.
Journal of the American College of Cardiology: Clinical Electrophysilogy, 2016 Dec [Epud ahead of print]; DOI: 10.1016/j.jacep.2016.10.011

Patton KK, Ellinor PT, Ezekowitz M, Kowey P, Lubitz SA, Perez M, Piccini J, Turakhia M, Wang P, Viskin S; American Heart Association Electrocardiography and Arrhythmias Committee of the Council on Clinical Cardiology and Council on Functional Genomics and Translational Biology. Electrocardiographic Early Repolarization: A Scientific Statement from the American Heart Association. Circulation. 2016 Apr 12;133(15):1520-9.

Perez MV, Uberoi A, Jain NA, Ashley E, Turakhia MP, Froelicher V. The prognostic value of early repolarization with ST-segment elevation in African Americans. Heart Rhythm 2012; 9:558.

Perrin MJ, Adler A, Green S, et al. Evaluation of genes encoding for the transient outward current (Ito) identifies the KCND2 gene as a cause of J wave syndrome associated with sudden cardiac death. Circ Cardiovasc Genet. 2014 Dec; 7(6):782-9.

Phillipson E, Herbert F. Accidental exposure to freezing: clinical and laboratory observations during convalescence from near-fatal hypothermia. Can Med Assoc J. 1967; 97:786-792.

Poelzing S, Akar FG, Baron E, Rosenbaum DS. Heterogeneous connexin43 expression produces electrophysiological heterogeneities across ventricular wall.
Am J Physiol Heart Circ Physiol 2004; 286:H2001–9.

Priori SG, Wilde AA, Horie M et al. HRS/EHRA/APHRS expert consensus statement on the diagnosis and management of patients with inherited primary arrhythmia syndromes: document endorsed by HRS, EHRA, and APHRS in May 2013 and by ACCF, AHA, PACES, and AEPC in June 2013. Heart Rhythm 2013; 10:1932–1963.

Ravens U, Wang XL, Wettwer E. Alpha adrenoceptor stimulation reduces outward currents in rat ventricular myocytes. J Pharmacol Exp Ther 1989; 250: 364-370

Reinhard W, Kaess BM, Debiec R, Nelson CP, Stark K, Tobin MD, Macfarlane PW, Tomaszewski M, Samani NJ, Hengstenberg C. Heritability of early repolarization: a population-based study. Circ Cardiovasc Genet 2011; 4:134–138.

Rollin A, Maury P, Bongard V, Sacher F, Delay M, Duparc A, Mondoly P, Carrie D, Ferrieres J, Ruidavets JB. Prevalence, prognosis, and identification of the malignant form of early repolarization pattern in a population-based study. Am J Cardiol. 2012; 110:1302–1308.

Rosati B, Pan Z, Lypen S, Wang HS, Cohen I, Dixon JE, McKinnon D. Regulation of KChIP2 potassium channel beta subunit gene expression underlies the gradient of transient outward current in canine and human ventricle. J Physiol 2001; 533:119–125.

Rosati B, Grau F, Rodriguez S, Li H, Nerbonne JM, McKinnon D. Concordant expression of KChIP2 mRNA, protein and transient outward current throughout the canine ventricle.
J Physiol 2003; 548:815–822.

Rosati B, Grau F, McKinnon D. Regional variation in mRNA transcript abundance within the ventricular wall. J. Mol. Cell Cardiol. 2006;40, 295e302.

Rosso R, Kogan E, Belhassen B, Rozovski U, Scheinman MM, Zeltser D, Halkin A, Steinvil A, Heller K, Glikson M, Katz A, Viskin S. J-point elevation in survivors of primary ventricular fibrillation and matched control subjects: incidence and clinical significance. J Am Coll Cardiol 2008; 52(15):1231–1238.

Rosso R, Glikson E, Belhassen B, Katz A, Halkin A, Steinvil A, Viskin S. Distinguishing "benign" from "malignant early repolarization": The value of the ST-segment morphology.
Heart Rhythm. 2012; 9:225–229.

Roten L, Derval N, Sacher F et al. Ajmaline attenuates electrocardiogram characteristics of inferolateral early repolarization. Heart Rhythm 2012; 9:232-239.

Rowley CP, Lobodzinski SS, Gold MR. The subcutaneous defibrillator.
Curr Treat Options Cardiovasc Med 2012;14:550-7

Sacher F, Derval N, Horlitz M, Haissaguerre M. J wave elevation to monitor quinidine efficacy in early repolarization syndrome. J Electrocardiol. 2014; 47:223–5.

Sacher F, Jesel L, Jais P, Haissaguerre M. Insight into the mechanism of Brugada syndrome: epicardial substrate and modification during ajmaline testing. Heart Rhythm 2014;11:732-734.

Sarkozy A and Dorian P. Anti-arrhythmic Drugs. In Principles of Medical Pharmacology. Edited by Kalant H, Grant DM and Mitchell J. Elsevier 2007, Canada, Toronto. pp. 430-447.

Sato D, Xie LH, Nguyen TP, Weiss JN, Qu Z. Irregularly appearing early afterdepolarizations in cardiac myocytes: Random fluctuations or dynamical chaos?
Biophysical journal. 2010;99:765-773

Shakur Y, Fong M, Hensley J, Cone J, Movsesian MA, Kambayashi J, Yoshitake M, Liu Y. Comparison of the effects of cilostazol and milrinone on cAMP-PDE activity, intracellular cAMP and calcium in the heart. Cardiovasc Drugs Ther 2002; 16:417–427.

Shinohara T, Ebata Y, Ayabe R, Fukui A, Okada N, Yufu K, Nakagawa M, Takahashi N. Combination therapy of cilostazol and bepridil suppresses recurrent ventricular fibrillation related to J-wave syndromes. Heart Rhythm. 2014; 11:1441–5.

Shinohara T, Kondo H, Otsubo T, Fukui A, Yufu K, Nakagawa M, Takahashi N.
Exaggerated Reactivity of Parasympathetic Nerves Is Involved in Ventricular Fibrillation in J-Wave Syndrome. J Cardiovasc Electrophysiol. 2016 Nov 25. doi: 10.1111/jce.13135. [Epub ahead of print]

Shipley RA, Hallaran WR. The four lead electrocardiogram in 200 normal men and women.
Am Heart J 1936; 11:325–345.

Shu J, Zhu T, Yang L, Cui C, Yan GX. ST-segment elevation in the early repolarization syndrome, idiopathic ventricular fibrillation, and the Brugada syndrome: cellular and clinical linkage. J Electrocardiol 2005; 38:26 – 32.

Singh S, Klein R, Eisenberg B, Hughes E, Shand M, and Doherty P. Long-term effect of mexiletine on left ventricular function and relation to suppression of ventricular arrhythmia. Am. J. Cardiol. 1990. 66(17): 1222-7. doi: 10.1016/0002-9149(90)91104-E. PMID: 1700592.

Sinner MF, Reinhard W, Muller M et al. Association of early repolarization pattern on ECG with risk of cardiac and all-cause mortality: a population-based prospective cohort study (MONICA/KORA). PLoS Med 2010; 7:e1000314.

Soltysinska E, Olesen SP, Christ T, Wettwer E, Varro A, Grunnet M, Jespersen T. Transmural expression of ion channels and transporters in human nondiseased and end-stage failing hearts. Pflugers Arch. 2009; 459, 11e23.

Sridharan MR, Horan LG. Electrocardiographic J wave of hypercalcemia. Am J Cardiol. 1984; 54:672-673.

Statland JM, Bundy BN, Wang Y, Rayan DR, Trivedi JR, Sansone VA, et al. Mexiletine for symptoms and signs of myotonia in nondystrophic myotonia: a randomized controlled trial. J.A.M.A. 2012; 308(13): 1357-65.

Szabo G, Szentandrassy N, Biro T, Toth BI, Czifra G, Magyar J, Banyasz T, Varro A, Kovacs L, Nanasi PP. Asymmetrical distribution of ion channels in canine and human left-ventricular wall: Epicardium versus midmyocardium. Pflugers Archiv: European journal of physiology. 2005; 450:307-316

Szentadrassy N, Banyasz T, Biro T, Szabo G, Toth BI, Magyar J, Lazar J, Varro A, Kovacs L, Nanasi PP. Apico-basal inhomogeneity in distribution of ion channels in canine and human ventricular myocardium. Cardiovascular research. 2005; 65:851-860.

Takagi M, Aonuma K, Sekiguchi Y, Yokoyama Y, Aihara N and Hiraoka M. The prognostic value of early repolarization (J wave) and ST-segment morphology after J wave in Brugada syndrome: Multicenter study in Japan. Heart Rhythm. 2013;10:533-539.

Tikkanen JT, Anttonen O, Junttila MJ, Aro AL, Kerola T, Rissanen HA, Reunanen A, Huikuri HV. Long-term outcome associated with early repolarization on electrocardiography.
N Engl J Med. 2009; 361(26):2529-37.

Tikkanen JT, Junttila MJ, Anttonen O, Aro AL, Luttinen S, Kerola T, Sager SJ, Rissanen HA, Myerburg RJ, Reunanen A, Huikuri HV. Early repolarization: electrocardiographic phenotypes associated with favorable long-term outcome. Circulation. 2011; 123:2666–2673.

Tomaszewski W. Changement electrocardiographiques observes chez un homme mort de froid. Arch Mal Coeur Vaiss 1938; 31:525–528.

Tran DX, Sato D, Yochelis A, Weiss JN, Garfinkel A, Qu Z. Bifurcation and chaos in a model of cardiac early afterdepolarizations. Physical review letters. 2009;102:258103

Van der Heyden MA, Wijnhoven TJ, Opthof T. Molecular aspects of adrenergic modulation of the transient outward current. Cardiovasc Res. 2006 Aug 1;71(3):430-42.

Varró A, Elharrar V, and Surawicz B. Frequency-dependent effects of several class I antiarrhythmic drugs on Vmax of action potential upstroke in canine cardiac Purkinje fibers. J. Cardiovasc. Pharmacol. 1985; 7(3): 482-92.

Varró A, and Lathrop DA. Sotalol and mexiletine: combination of rate-dependent electrophysiological effects. J. Cardiovasc. Pharmacol. 1990; 16(4): 557-67.

Vaughan Williams EM. Class 1 Antiarrhytmic Action. In Control of Cardiac Rhythm. 1998. Edited by E.M. Vaughan Willams and J.C. Somberg. Lippincott-Raven Publishers, Philadelphia. pp. 11-32.

Wagner WL, Manz M, Lüderitz B. Kombination von Sotalol mit den Klasse-I-B Substanzen Mexiletin oder Tocainid bei Komplexer ventrikulärer Extrasystolie. Z Kardiol 1987; 76:296-302.

Wasserburger RH, Alt WJ. The normal RS-T segment elevation variant. Am J Cardiol 1961; 8:184 –192.

Watanabe H, Nogami A, Ohkubo K, et al. Electrocardiographic characteristics and SCN5A mutations in idiopathic ventricular fibrillation associated with early repolarization. Circ Arrhythm Electrophysiol 2011;4:874-881.

Watanabe H, Ohkubo K, Watanabe I, Matsuyama TA, Ishibashi-Ueda H, Yagihara N, Shimizu W, Horie M, MinaminoT, Makita N. SCN5A mutation associated with ventricular fibrillation, early repolarization, and concealed myocardial abnormalities. Int J Cardiol 2013; 165:e21–e23.

Watanabe M, Otani NF, Gilmour RF, Jr. Biphasic restitution of action potential duration and complex dynamics in ventricular myocardium. Circulation research. 1995; 76:915-921

Weiss MD, Macklin EA, Simmons Z, Knox AS, Greenblatt DJ, Atassi N, et al. A randomized trial of mexiletine in ALS: Safety and effects on muscle cramps and progression. Neurology 2016; 86(16): 1474-81.

Xie Y, Hu G, Sato D, Weiss JN, Garfinkel A, Qu Z. Dispersion of refractoriness and induction of reentry due to chaos synchronization in a model of cardiac tissue. Physical review letters. 2007; 99:118101

Xie Y, Sato D, Garfinkel A, Qu Z, Weiss JN. So little source, so much sink: requirements for afterdepolarizations to propagate in tissue. Biophys J. 2010;99:1408–15.

Yamada KA, Kanter EM, Green KG, Saffitz JE. Transmural distribution of connexins in rodent hearts. J Cardiovasc Electrophysiol 2004; 15: 710–5.

Yamaguchi I, Singh BN, and Mandel WJ. Electrophysiological actions of mexiletine on isolated rabbit atria and canine ventricular muscle and purkinje fibres. Cardiovasc. Res. 1979; 13(5): 288-96.

Yan GX, Antzelevitch C. Cellular basis for the electrocardiographic J wave. Circulation 1996; 93:372–379.

Yan GX, Shimizu W, Antzelevitch C. Characteristics and distribution of M cells in arterially-perfused canine left ventricular wedge preparations. Circulation 1998;98:1921–7.

Yan GX, Antzelevitch C. Cellular basis for the Brugada syndrome and other mechanisms of arrhythmogenesis associated with ST-segment elevation. Circulation. 1999;100(15):1660-6.

Zicha S, Xiao L, Stafford S, Cha TJ, Han W, Varro A, Nattel S. Transmural expression of transient outward potassium current subunits in normal and failing canine and human hearts. J Physiol 2004; 561:735–748.

ZygmuntAC, GoodrowRJ, Antzelevitch C. Sodium effects on 4-aminopyridine- sensitive transient outward current in canine ventricular cells. Am J Physiol 1997; 272:H1–H11.

.